Author's personal copy

Easlon, E., Tsang, F., Skinner, C., Wang, C., Lin, S.J., 2008. The malate-aspartate NADH shuttle components are novel metabolic longevity regulators required for calorie restriction-mediated life span extension in yeast. Genes Dev. 22, 931–944.
Farmer, S.R., 2006. Transcriptional control of adipocyte formation. Cell Metab. 4, 263–273.
Farmer, S.R., 2008. Molecular determinants of brown adipocyte formation and function. Genes Dev. 22, 1269–1275.
Frayn, K.N., 2002. Adipose tissue as a buffer for daily lipid flux. Diabetologia 45, 1201–1210.
Gnacińska, M., Małgorzewicz, S., Stojek, M., Łysiak-Szydłowska, W., Sworczak, K., 2009. Role of adipokines in complications related to obesity: a review. Adv. Med. Sci. 54, 150–157.
Griffin, M.J., Sul, H.S., 2004. Insulin regulation of fatty acid synthase gene transcription: roles of USF and SREBP-1c. IUBMB Life 56, 595–600.
Guay, C., Madiraju, S.R., Aumais, A., Joly, E., Prentki, M., 2007. A role for ATP-citrate lyase, malic enzyme, and pyruvate/citrate cycling in glucose-induced insulin secretion. J. Biol. Chem. 282, 35657–35665.
Higami, Y., Pugh, T.D., Page, G.P., Allison, D.B., Prolla, T.A., Weindruch, R., 2004. Adipose tissue energy metabolism: altered gene expression profile of mice subjected to long-term caloric restriction. FASEB J. 18, 415–417.
Higami, Y., Yamaza, H., Shimokawa, I., 2005. Laboratory findings of caloric restriction in rodents and primates. Adv. Clin. Chem. 39, 211–237.
Higami, Y., Barger, J.L., Page, G.P., Allison, D.B., Smith, S.R., Prolla, T.A., Weindruch, R., 2006a. Energy restriction lowers the expression of genes linked to inflammation, the cytoskeleton, the extracellular matrix, and angiogenesis in mouse adipose tissue. J. Nutr. 136, 343–352.
Higami, Y., Tsuchiya, T., Chiba, T., Yamaza, H., Muraoka, I., Hirose, M., Komatsu, T., Shimokawa, I., 2006b. Hepatic gene expression profile of lipid metabolism in rats: Impact of caloric restriction and growth hormone/insulin-like growth factor-1 suppression. J. Gerontol. A: Biol. Sci. Med. Sci. 61, 1099–1110.
Hotamisligil, G.S., Arner, P., Caro, J.F., Atkinson, R.L., Spiegelman, B.M., 1995. Increased adipose tissue expression of tumor necrosis factor-alpha in human obesity and insulin resistance. J. Clin. Invest. 95, 2409–2415.
Huh, T.L., Casazza, J.P., Huh, J.W., Chi, Y.T., Song, B.J., 1990. Characterization of two cDNA clones for pyruvate dehydrogenase E1 beta subunit and its regulation in tricarboxylic acid cycle-deficient fibroblast. J. Biol. Chem. 265, 13320–13326.
Ikeda, Y., Okamura-Ikeda, K., Tanaka, K., 1985. Purification and characterization of short-chain, medium-chain, and long-chain acyl-CoA dehydrogenases from rat liver mitochondria. Isolation of the holo- and apoenzymes and conversion of the apoenzyme to the holoenzyme. J. Biol. Chem. 260, 1311–1325.
Ikegami, K., Setou, M., 2009. TTLL10 can perform tubulin glycylation when co-expressed with TTLL8. FEBS Lett. 583, 1957–1963.
Jahnke, V.E., Sabido, O., Defour, A., Castells, J., Lefai, E., Roussel, D., Freyssenet, D., 2010. Evidence for mitochondrial respiratory deficiency in rat rhabdomyosarcoma cells. PLoS One 5, e8637.
Jensen, M.V., Joseph, J.W., Ronnebaum, S.M., Burgess, S.C., Sherry, A.D., Newgard, C.B., 2008. Metabolic cycling in control of glucose-stimulated insulin secretion. Am. J. Physiol. Endocrinol. Metab. 295, E1287–E1297.
Jitrapakdee, S., Vidal-Puig, A., Wallace, J.C., 2006. Anaplerotic roles of pyruvate carboxylase in mammalian tissues. Cell. Mol. Life Sci. 63, 843–854.
Kang, D., Kim, S.H., Hamasaki, N., 2007. Mitochondrial transcription factor A (TFAM): roles in maintenance of mtDNA and cellular functions. Mitochondrion 7, 39–44.
Katic, M., Kennedy, A.R., Leykin, I., Norris, A., McGettrick, A., Gesta, S., Russell, S.J., Bluher, M., Maratos-Flier, E., Kahn, C.R., 2007. Mitochondrial gene expression and increased oxidative metabolism: role in increased lifespan of fat-specific insulin receptor knock-out mice. Aging Cell 6, 827–839.
Kenyon, C., 2005. The plasticity of aging: insights from long-lived mutants. Cell 120, 449–460.
Kerscher, S., Dröse, S., Zickermann, V., Brandt, U., 2008. The three families of respiratory NADH dehydrogenases. Results Probl. Cell Differ. 45, 185–222.
Koekemoer, T.C., Downing, T.G., Oelofsen, W., 1998. An alternative PCR assay for quantifying mitochondrial DNA in crude preparations. Nucleic Acids Res. 26, 2829–2830.
Lambeth, D.O., Tews, K.N., Adkins, S., Frohlich, D., Milavetz, B.I., 2004. Expression of two succinyl-CoA synthetases with different nucleotide specificities in mammalian tissues. J. Biol. Chem. 279, 36621–36624.
Lenka, N., Vijayasarathy, C., Mullick, J., Avadhani, N.G., 1998. Structural organization and transcription regulation of nuclear genes encoding the mammalian cytochrome c oxidase complex. Prog. Nucleic Acid Res. Mol. Biol. 61, 309–344.
Liang, H., Ward, W.F., 2006. PGC-1alpha: a key regulator of energy metabolism. Adv. Physiol. Educ. 30, 145–151.
Masoro, E.J., 2005. Overview of caloric restriction and ageing. Mech. Ageing Dev. 126, 913–922.
Nakamura, M., Yamada, M., Ohsawa, T., Morisawa, H., Nishine, T., Nishimura, O., Toda, T., 2006. Phosphoproteomic profiling of human SH-SY5Y neuroblastoma cells during response to 6-hydroxydopamine-induced oxidative stress. Biochim. Biophys. Acta 1763, 977–989.
Nisoli, E., Tonello, C., Cardile, A., Cozzi, V., Bracale, R., Tedesco, L., Falcone, S., Valerio, A., Cantoni, O., Clementi, E., Moncada, S., Carruba, M.O., 2005. Calorie restriction promotes mitochondrial biogenesis by inducing the expression of eNOS. Science 310, 314–317.
Otabe, S., Yuan, X., Fukutani, T., Wada, N., Hashinaga, T., Nakayama, H., Hirota, N., Kojima, M., Yamada, K., 2007. Overexpression of human adiponectin in transgenic mice results in suppression of fat accumulation and prevention of premature death by high-calorie diet. Am. J. Physiol. Endocrinol. Metab. 293, E210–E218.
Puigserver, P., Spiegelman, B.M., 2003. Peroxisome proliferator-activated receptor-gamma coactivator 1 alpha (PGC-1 alpha): transcriptional coactivator and metabolic regulator. Endocr. Rev. 24, 78–90.
Ramakrishna, S., Benjamin, W.B., 1979. Fat cell protein phosphorylation. Identification of phosphoprotein-2 as ATP-citrate lyase. J. Biol. Chem. 254, 9232–9236.
Saely, C.H., Geiger, K., Drexel, H., 2010. Brown versus white adipose tissue: a mini-review. Gerontology [Epub ahead of print].
Sakai, T., Sakaue, H., Nakamura, T., Okada, M., Matsuki, Y., Watanabe, E., Hiramatsu, R., Nakayama, K., Nakayama, K.I., Kasuga, M., 2007. Skp2 controls adipocyte proliferation during the development of obesity. J. Biol. Chem. 282, 2038–2046.
Salway, T.G., 1999. Metabolism at a Glance, 2nd ed. Blackwell Science Ltd., Oxford, UK.
She, P., Van Horn, C., Reid, T., Hutson, S.M., Cooney, R.N., Lynch, C.J., 2007. Obesity-related elevations in plasma leucine are associated with alterations in enzymes involved in branched-chain amino acid metabolism. Am. J. Physiol. Endocrinol. Metab. 293, E1552–E1563.
Shi, T., Wang, F., Stieren, E., Tong, Q., 2005. SIRT3, a mitochondrial sirtuin deacetylase, regulates mitochondrial function and thermogenesis in brown adipocytes. J. Biol. Chem. 280, 13560–13567.
Sinclair, D.A., 2005. Toward a unified theory of caloric restriction and longevity regulation. Mech. Ageing Dev. 126, 987–1002.
Stofkova, A., 2009. Leptin and adiponectin: from energy and metabolic dysbalance to inflammation and autoimmunity. Endocr. Regul. 43, 157–168.
Sugden, M.C., Holness, M.J., 2003. Recent advances in mechanisms regulating glucose oxidation at the level of the pyruvate dehydrogenase complex by PDKs. Am. J. Physiol. Endocrinol. Metab. 284, E855–E862.
Taroni, F., Di Donato, S., 1988. Purification and properties of cytosolic malic enzyme from human skeletal muscle. Int. J. Biochem. 20, 857–866.
Torres-Leal, F.L., Fonseca-Alaniz, M.H., Rogero, M.M., Tirapegui, J., 2010. The role of inflamed adipose tissue in the insulin resistance. Cell Biochem. Funct. 28, 623–631.
Valle, A., Sastre-Serra, J., Roca, P., Oliver, J., 2010. Modulation of white adipose tissue proteome by aging and calorie restriction. Aging Cell 9, 882–894.
Wang, X., Paigen, B., 2005. Genetics of variation in HDL cholesterol in humans and mice. Circ. Res. 96, 27–42.
Watford, M., 2000. Functional glycerol kinase activity and the possibility of a major role for glyceroneogenesis in mammalian skeletal muscle. Nutr. Rev. 58, 145–148.
Weindruch, R., Walford, R.L., 1988. The Retardation of Aging and Disease by Dietary Restriction. Charles C Thomas Publisher, Springfield, IL.
Wiegand, G., Remington, S.J., 1986. Citrate synthase: structure control, and mechanism. Annu. Rev. Biophys. Biophys. Chem. 15, 97–117.
Yamauchi, T., Kamon, J., Waki, H., Terauchi, Y., Kubota, N., Hara, K., Mori, Y., Ide, T., Murakami, K., Tsuboyama-Kasaoka, N., Ezaki, O., Akanuma, Y., Gavrilova, O., Vinson, C., Reitman, M.L., Kagechika, H., Shudo, K., Yoda, M., Nakano, Y., Tobe, K., Nagai, R., Kimura, S., Tomita, M., Froguel, P., Kadowaki, T., 2001. The fat-derived hormone adiponectin reverses insulin resistance associated with both lipoatrophy and obesity. Nat. Med. 7, 941–946.
Yamauchi, T., Kamon, J., Minokoshi, Y., Ito, Y., Waki, H., Uchida, S., Yamashita, S., Noda, M., Kita, S., Ueki, K., Eto, K., Akanuma, Y., Froguel, P., Foufelle, F., Ferre, P., Carling, D., Kimura, S., Nagai, R., Kahn, B.B., Kadowaki, T., 2002. Adiponectin stimulates glucose utilization and fatty-acid oxidation by activating AMP-activated protein kinase. Nat. Med. 8, 1288–1295.
Yamaza, H., Komatsu, T., To, K., Toyama, H., Chiba, T., Higami, Y., Shimokawa, I., 2007. Involvement of insulin-like growth factor-1 in the effect of caloric restriction: regulation of plasma adiponectin and leptin. J. Gerontol. A: Biol. Sci. Med. Sci. 62, 27–33.
Yu, B.P., 1994. Modulation of Aging Processes by Dietary Restriction. CRC Press, Boca Raton, FL.
Zhu, M., Lee, G.D., Ding, L., Hu, J., Qiu, G., de Cabo, R., Bernier, M., Ingram, D.K., Zou, S., 2007. Adipogenic signaling in rat white adipose tissue: modulation by aging and calorie restriction. Exp. Gerontol. 42, 733–744.

AGE
DOI 10.1007/s11357-012-9439-1

Caloric restriction-associated remodeling of rat white adipose tissue: effects on the growth hormone/insulin-like growth factor-1 axis, sterol regulatory element binding protein-1, and macrophage infiltration

Yoshikazu Chujo · Namiki Fujii · Naoyuki Okita · Tomokazu Konishi · Takumi Narita · Atsushi Yamada · Yushi Haruyama · Kosuke Tashiro · Takuya Chiba · Isao Shimokawa · Yoshikazu Higami

Received: 27 December 2011 / Accepted: 16 May 2012
© American Aging Association 2012

Abstract The role of the growth hormone (GH)-insulin-like growth factor (IGF)-1 axis in the lifelong caloric restriction (CR)-associated remodeling of white adipose tissue (WAT), adipocyte size, and gene expression profiles was explored in this study. We analyzed the WAT morphology of 6–7-month-old wild-type Wistar rats fed ad libitum (WdAL) or subjected to CR (WdCR), and of heterozygous transgenic dwarf rats bearing an anti-sense GH transgene fed ad libitum (TgAL) or subjected to CR (TgCR). Although less effective in TgAL, the adipocyte size was significantly reduced in WdCR compared with WdAL. This CR effect was blunted in Tg rats. We also used high-density oligonucleotide microarrays to examine the gene expression profile of WAT of WdAL, WdCR, and TgAL rats. The gene expression profile of WdCR, but not TgAL, differed greatly from that of WdAL. The gene clusters with the largest changes induced by CR but not by Tg were genes involved in lipid biosynthesis and inflammation, particularly sterol regulatory element binding proteins (SREBPs)-regulated and macrophage-related genes, respectively. Real-time reverse-transcription polymerase chain reaction analysis confirmed that the expression of *SREBP-1* and its downstream targets was upregulated, whereas the macrophage-related genes were downregulated in WdCR, but not in TgAL. In addition, CR affected the gene expression profile of Tg rats similarly to wild-type rats. Our findings suggest that CR-associated remodeling of WAT, which involves SREBP-1-mediated transcriptional activation and suppression of macrophage infiltration, is regulated in a GH–IGF-1-independent manner.

Yoshikazu Chujo, Namiki Fujii, Naoyuki Okita, and Tomokazu Konishi contributed equally to this work.

Electronic supplementary material The online version of this article (doi:10.1007/s11357-012-9439-1) contains supplementary material, which is available to authorized users.

Y. Chujo · N. Fujii · N. Okita · T. Narita · A. Yamada · Y. Haruyama · Y. Higami (✉)
Molecular Pathology and Metabolic Disease, Faculty of Pharmaceutical Sciences, Tokyo University of Science, Chiba, Japan
e-mail: higami@rs.noda.tus.ac.jp

T. Konishi
Molecular Genetics Group, Akita Prefectural University, Akita, Japan

K. Tashiro
Graduate School of Bioresource and Bioenvironmental Sciences, Molecular Gene Technics, Kyushu University, Fukuoka, Japan

T. Chiba · I. Shimokawa
Department of Investigative Pathology, Nagasaki University Graduate School of Biomedical Sciences, Nagasaki, Japan

Published online: 28 May 2012

Keywords Growth hormone · Insulin-like growth factor-1 · Caloric restriction (CR) · Lipid biosynthesis · Sterol regulatory element binding protein · DNA microarray

Introduction

Ames and Snell mutant dwarf mice, which lack growth hormone (GH), prolactin, and thyroid-stimulating hormone, live approximately 20–50 % longer than wild-type mice (Brown-Borg et al. 1996; Flurkey et al. 2001). Similarly, disrupted GH receptor/binding protein (GHR/BP) knockout (KO) mice live significantly longer than their wild-type controls (Coschigano et al. 2000). The longevity of heterozygous insulin-like growth factor (IGF)-1 receptor KO mice, and both heterozygous and homozygous insulin receptor substrate-1 KO mice (particularly females) show markedly extended lifespan compared with their counterparts (Holzenberger et al. 2003). We have also reported that heterozygous transgenic dwarf rats, bearing an anti-sense GH transgene, live longer than controls (Shimokawa et al. 2002). Based on these studies, the GH–IGF-1 axis and/or its related signaling pathways are important lifespan regulators (Bartke 2005).

Although new genetic interventions that extend the lifespan of mammals are emerging, caloric restriction (CR) remains the most robust, reproducible, and simple experimental manipulation known to extend both median and maximum lifespan, and to delay the onset of many age-associated pathophysiological changes in laboratory rodents (Weindruch and Walford 1988; Yu 1994). In general, attenuation of oxidative and other stresses, the modulation of glycemia and insulinemia, and the activation of sirtuin may be significant factors in the beneficial effects of CR (Weindruch and Walford 1988; Yu 1994; Sohal and Weindruch 1996; Masoro 2005; Sinclair 2005). Moreover, Nisoli et al. (2005) suggested that the enhanced mitochondrial biogenesis is also involved in the beneficial action of CR. Thereafter, several investigators reported that CR induces mitochondrial biogenesis (Anderson and Prolla 2009; López-Lluch et al. 2006; Shi et al., 2005). On the other hand, Hancock et al. (2011) and Gesing et al. (2011) demonstrated that CR does not increase it. Recently, we also reported that CR enhances mitochondrial biogenesis in white adipose tissue (WAT) but not in brown adipose tissue (Okita et al. 2012). Thus, the exact mechanisms underlying CR are still debated. CR animals share many characteristics with long-living dwarf mice, including smaller body size, and lower plasma insulin and IGF-1 levels (Sinclair 2005; Al-Regaiey et al. 2005). CR does not further extend the lifespan of the already long-lived GHR/BP KO mice (Bonkowski et al. 2006). In contrast, CR further extends the longevity of Ames dwarf mice and heterozygous transgenic dwarf rats bearing an anti-sense GH transgene, which live longer than their wild-type controls (Bartke et al. 2001; Shimokawa et al. 2003). Therefore, the beneficial effects of CR are not solely dependent on the GH–IGF-1 axis. In terms of the hepatic gene expression profile, CR mainly alters the expression of genes involved in the stress response, xenobiotic metabolism, and lipid metabolism. Most genes involved in stress response and xenobiotic metabolism are regulated in a GH–IGF-1-dependent manner, while those involved in lipid metabolism are regulated in a GH–IGF-1-independent manner. Moreover, CR enhances the expression of genes involved in fatty acid synthesis after feeding, and of genes encoding mitochondrial β-oxidation enzymes during food shortage, probably via transcriptional regulation by sterol regulatory element binding protein 1 (SREBP-1) and peroxisome proliferator-activated receptor (PPAR)-α, respectively (Higami et al. 2006b). Considering these findings together with serum biochemical parameters, we proposed that CR enhances lipid utilization via hepatic transcriptional changes and prevents hepatic steatosis in a GH–IGF-1-independent manner (Higami et al. 2006b).

Adipose tissue plays a central role in the regulation of both energy storage and expenditure (Saely et al. 2012). Numerous WAT-derived secretory molecules, including leptin, tumor necrosis factor (TNF)-α, and adiponectin, have been characterized, and some of these molecules play significant roles in obesity and insulin resistance (Torres-Leal et al. 2010; Ouchi et al. 2011). Therefore, WAT is now recognized as an endocrine organ rather than an inert tissue, and is implicated in the pathogenesis and complications of type 2 diabetes. It has been reported that fat-specific insulin receptor knockout mice live longer than their controls (Blüher et al. 2003). These mice show reduced adiposity and altered secretion of adipokines, including higher adiponectin and lower pro-inflammatory cytokine levels (Blüher et al. 2002). The transcription factors C/EBPα, C/EBPβ, and PPARγ are master regulators of adipocyte differentiation (Farmer 2006). Mice in which C/EBPα is replaced with C/EBPβ (β/β

mice) live longer and have reduced adiposity compared with their wild-type controls (Chiu et al. 2004). In contrast, hetero-deficient PPARγ KO mice have a shortened lifespan (Argmann et al. 2009). Transgenic mice expressing adiponectin in the liver live longer than controls, and are resistant to high-calorie diet-induced obesity (Otabe et al. 2007). Thus, altered adipose tissue gene expression and modulation of adipokine secretion seem to influence the lifespan of rodents. CR reduces adiposity and reduces adipocyte size by altering the gene expression profile (Higami et al. 2004, 2006a). CR decreases plasma insulin and leptin levels, and increases plasma adiponectin levels (Higami et al. 2005; Yamaza et al. 2007). CR also reverses age-associated insulin resistance, possibly by decreasing adiposity (Barzilai et al. 1998). Moreover, Masternak et al. (2012) reported that visceral fat removal improved insulin sensitivity, suppressed fat accumulation in the skeletal muscle, and reduced body temperature and respiratory quotient in wild-type mice and had opposite effects on long-living GHR/BP KO mice. Therefore, we hypothesized that the beneficial actions of CR may be partially mediated by WAT remodeling as well as decreasing adiposity.

In the present study, to explore the role of the GH–IGF-1 axis in CR-associated remodeling of WAT, we compared adipocyte size and gene expression profiles of WAT between CR rats and transgenic dwarf rats, bearing an anti-sense GH transgene. We propose that CR-associated remodeling of WAT, which is transcriptionally regulated by SREBP-1 and modulated by macrophage infiltration, could be regulated in a GH–IGF-1-independent manner.

Materials and Methods

Animals

The present study was conducted in accordance with the provisions of the Ethics Review Committee for Animal Experimentation at Nagasaki University. The rat characteristics and animal care are described elsewhere (Higami et al. 2006a). Briefly, in this study we used ad libitum (AL)-fed male heterozygous transgenic dwarf rats, bearing the anti-sense growth hormone transgene (tg/−; Tg), and their genetic background, Jcl:Wistar (−/−; wild-type) rats. From 6 weeks of age, both wild-type and Tg rats were divided into two groups: AL and CR (70 % of the energy intake). CR was started without adjustment for food shortage. CR rats were fed every other day. Their 2-day food allotment was equal to 140 % of the mean daily intake of AL rats. Wild-type AL (WdAL) and CR (WdCR), and Tg AL (TgAL) and CR (TgCR) rats were killed at 6–7 months of age. The day before the rats were killed, they were all provided with their allocated food 30 min before the lights were turned off in the evening and were killed after the lights were turned on the following morning. Thus, all rats were not under fasting condition when killed. Immediately after killing the rats, epididymal white adipose tissue (WAT) was collected and its weight was measured. Some of the isolated WAT was fixed in a buffered formalin solution for histological examination and the rest was immediately diced, frozen in liquid nitrogen, and stored at −80°C. Total RNA was extracted from the stored WAT for DNA microarray analysis and quantitative real-time reverse-transcription polymerase chain reaction (RT-PCR).

Histological examination

Fixed tissues were processed routinely and embedded in paraffin. Tissue sections (5 μm thick) were stained with hematoxylin–eosin. The stained sections were scanned by microscopy with a charge-coupled device camera (Nikon, Tokyo, Japan). All images were recorded after precise focusing. ImageJ 1.43u/Java1.6.0_22 software was used for all tissue analyses. The size distribution of each white area in the black-and-white images, corresponding to lipid droplets, was counted and calculated. To avoid inter-rater variation, a single observer (YC) carried out tissue analyses.

Microarrays and data normalization

Total RNA was measured using an Affymetrix Rat Genome 230_2.0 GeneChip (Affymetrix, Santa Clara, CA, USA), with four biological repeats per group. The raw data were deposited in Gene Expression Omnibus (accession code: GSE30668). The perfect match data were normalized and the expression levels of each gene were estimated using the SuperNORM data service (Skylight Biotech Inc., Akita, Japan) according to a three-parameter log-normal distribution model (Konishi et al. 2008). To reduce noise effects, the analyses were focused on genes identified as positive by two-way analysis of variance (ANOVA), with a two-sided threshold of 0.001. Out of 31,099 genes on each chip, 6,641 were positive.

Principal component analysis

To compare the effects of CR (WdAL vs. WdCR) with those of Tg (WdAL vs. TgAL), we performed principal component (PC) analysis (Jackson 2005) on the ANOVA-positive genes. To reduce the effects of individual differences between samples, the axes of the PC analysis were estimated on a matrix of each group's sample means and applied to all data, which were centered using the sample means of WdAL rats (the R scripts used are available in the Supplemental Materials and Methods). The methodology rotated the original data matrix around the center of the WdAL rats, to fit perpendicular axes toward which most of the variations in the data appeared. The distribution of each PC value was checked on a normal QQ plot and outlier genes that departed from the normality (PC1: >0.16 and < –016 in Supplemental Fig. 1; PC2: >0.1 and < –0.1 in Supplemental Fig. 2) were selected.

Evaluation of frequently occurring biological functions in gene annotations

To test the significance among categories of biological functions that appeared in the selected genes' annotations, we applied binomial statistical tests based on the frequencies found in the Gene Ontology (GO) Biological Process annotations (release 31) provided by Affymetrix (Konishi et al. 2008).

Quantitative real-time RT-PCR

To obtain cDNA, 1 μg of RNA extracted from WAT of WdAL, WdCR, TgAL, and TgCR rats was reverse transcribed using PrimeScript Reverse Transcriptase (Takara, Shiga, Japan) with random hexamers (Takara). Quantitative real-time PCR was performed using an Applied Biosystems 7300 real-time PCR system (Applied Biosystems, Carlsbad, CA, USA) with SYBR Premix ExTaqII (Takara). The primer sequences for *SREBP-1a*, *SREBP-1c*, *SREBP-2*, *fatty acid synthase* (*FASN*), *acetyl-CoA carboxylase 1* (*ACC1*), *squalene epoxidase* (*Sqle*), *mevalonate kinase* (*Mvk*), *F4/80*, *monocyte chemotactic protein-1* (*MCP-1*), *CD11c* (also known as *integrin alpha X*), *CD163*, and *TATA box binding protein* (*TBP*) are shown in Table 1. TBP was used as a normalization control. The amount of target mRNA relative to *TBP* mRNA in the three groups was obtained. Data from three to six rats per group are expressed as means±SEM and were compared using Tukey's *t* test. Differences were considered statistically significant at $P<0.05$.

Results

CR markedly reduced the body weight of both wild-type and Tg rats. Tg also significantly decreased the body weight of both AL and CR rats (WdAL, 486.9± 29.9 g; WdCR, 349.7±15.6 g; TgAL, 310.3±12.1 g; TgCR, 237.8±25.7 g). Similarly, CR markedly reduced the epididymal WAT weight of both wild-type and Tg rats. Tg also significantly reduced it in both AL and CR rats (WdAL, 7.02±1.04 g; WdCR, 4.96± 0.97 g; TgAL, 4.76±0.74 g; TgCR, 4.32±0.88 g). In contrast, WAT weight as a percentage of body weight, which represents adiposity, did not differ among WdAL, WdCR, and TgAL rats, but it was markedly increased in TgCR rats (WdAL, 1.44± 0.18 %; WdCR, 1.42±0.27 %; TgAL, 1.53± 0.22 %; TgCR, 1.81±0.26 %).

CR significantly reduced the size of white adipocytes, but this effect was predominantly found in wild-type rats compared with Tg rats (Fig. 1a–d). Tg also slightly reduced their size, but it was likely that the effect of Tg was less than that of CR (Fig. 1a and c). In fact, the median adipocyte size was significantly smaller in WdCR than in WdAL, but not in TgCR compared with TgAL. It was slightly but significantly smaller in TgAL than in WdAL (WdAL vs. WdCR: $p=0.001$, TgAL vs. TgCR: $p=0.100$, WdAL vs. TgAL: $p=0.026$, Fig. 1f). The percentage of adipocytes showing >5,000 μm^2 was also significantly lower in WdCR than WdAL, but not in TgCR compared with TgAL. It was slightly but significantly smaller in TgAL than in WdAL (WdAL vs. WdCR: $p<0.001$, TgAL vs. TgCR: $p=0.090$, WdAL vs. TgAL: $p=0.039$, Fig. 1g). In WAT of WdCR and TgCR, the adipocytes were predominantly 1,000–3,000 μm^2 in area, whereas those in WdAL and TgAL WAT showed a much greater size distribution. This pattern was more significant in WdAL than in TgAL rats (Fig. 1e).

Based on the DNA microarray data of WdAL, WdCR, and TgAL, using high-density oligonucleotide microarrays, 6,641 genes were positive based on two-way ANOVA ($P<0.001$). These genes were applied to PC analysis. The PC scores for each group and their

Table 1 List of primers for real-time RT-PCR

	Forward	Reverse
SREBP-1a[a]	5′-CCGAGGTGTGCGAAATGG-3′	5′-TTGATGAGCTGAAGCATGTCTTC-3′
SREBP-1c[b]	5′-GGAGCCATGGATTGCACATT-3′	5′-GGCCCGGGAAGTCACTGT-3′
SREBP-2	5′-CGATCAAGTCAGCAGCCAAG-3′	5′-AATCCCACAGAGTCCACAAAAG-3′
FASN	5′-AGCAGGCACACACAATGGAC-3′	5′-GAAGAAGAAAGAGAGCCGGTTG-3′
ACC1	5′-TGGATGAACCATCTCCGTTG-3′	5′-CATGTGAAAGGCCAAACC-3′
Sqle	5′-GTCTCCGGAAAGCAGCTATGG-3′	5′-CTCCTTGGTGTCCCCAGTCTC-3′
Mvk	5′-CAGAGCAATGGGAAAGTGAGC-3′	5′-TCTCCAGTTGCTCCAAGGTG-3′
MCP-1	5′-CCAGCCAACTCTCACTGAAGC-3′	5′-CTTCTTTGGGACACCTGCTG-3′
F4/80	5′-GGCCAAGATTCTCTTCCTCAC-3′	5′-TCACCACCTTCAGGTTTCTCAC-3′
CD11c	5′-AGCACACGGGGAAGGTTGTC-3′	5′-CAGGTCAGTGCTGCCATCTCTATC-3′
CD163	5′-ACAAATACGTGGCTCTTTCCTG-3′	5′-ATGGGATTTCTCCTCCAACC-3′
TBP	5′-CAGTACAGCAATCAACATCTCAGC-3′	5′-CAAGTTTACAGCCAAGATTCACG-3′

[a] Koo et al. (2009)

[b] Yang et al. (2001)

gene expressions are shown in a scatter plot (Fig. 2a). The PC1 and PC2 axes almost coincided with the effects of CR (WdAL vs. WdCR) and Tg (WdAL vs. TgAL), respectively. CR was more effective than Tg because the gene expression plots were more widely distributed along the PC1 axis than the PC2 axis. Indeed, 199 and 226 genes showing PC1 >0.16 and PC1 < –0.16 were upregulated and downregulated by CR, respectively. In contrast, only 65 and 118 genes showing PC2 >0.1 and PC2 < –0.1 were upregulated and downregulated by Tg, respectively (Table 2). Binomial tests were performed using the selected genes

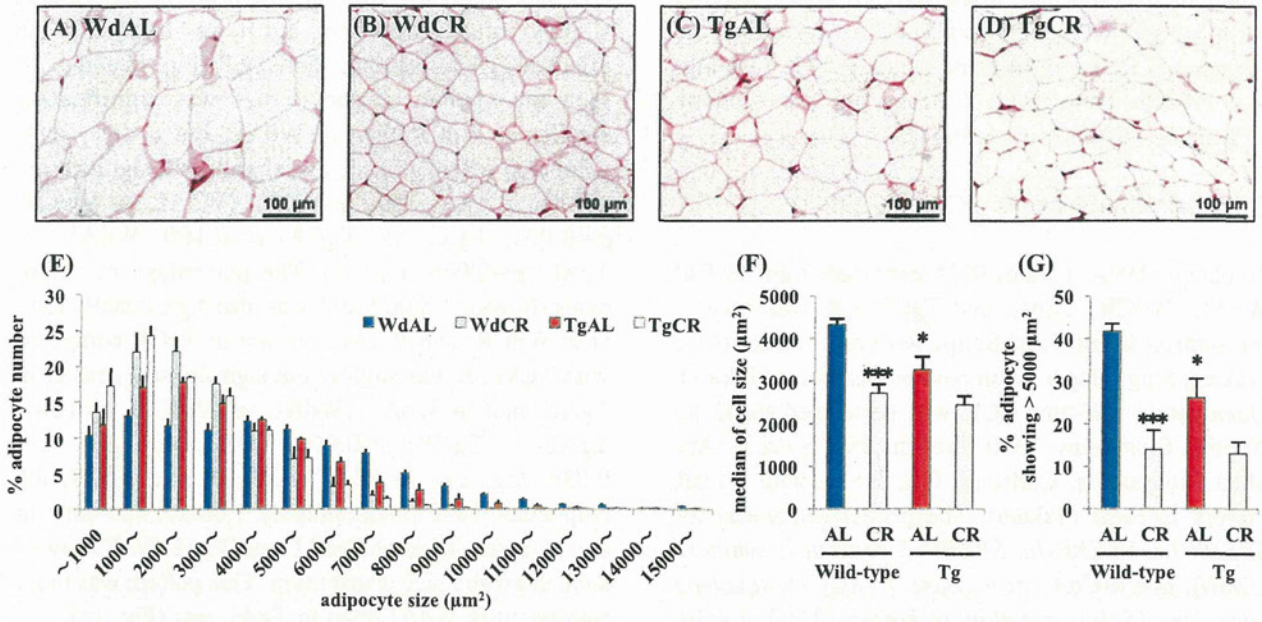

Fig. 1 Effects of CR and Tg on morphologic features of white adipose tissue. Representative hematoxylin/eosin-stained histological sections of WAT from WdAL (**a**), WdCR (**b**), TgAL (**c**), and TgCR (**d**) rats (magnification ×40; *scale bar* 100 μm). **e** Distribution of adipocyte sizes in wild-type and tg rats. **f** Median of adipocyte sizes in wild-type and Tg rats. **g** The percentage of adipocytes showing >5,000 μm² in wild-type and Tg rats. Adipocyte size was calculated based on a quantitative morphometric method using ImageJ 1.43u/Java1.6.0_22 software. *Error bars* are SEM for each group (n=4). Approximately 1,000–2,100 adipocytes were counted per rat. *P<0.05 and ***P< 0.001 vs. WdAL (Tukey's t test)

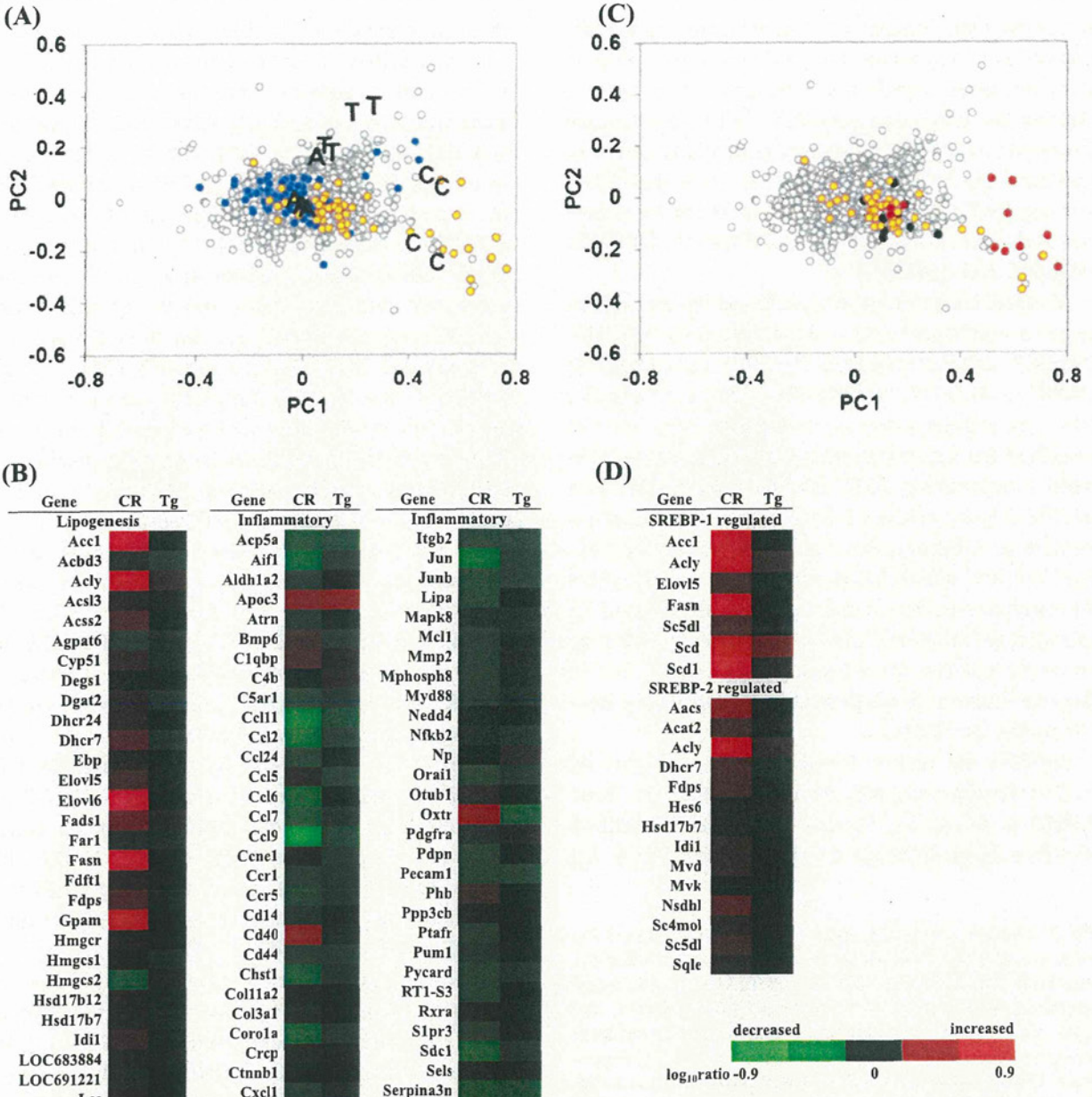
(A)
PC2
PC1
0.6
0.4
0.2
0
-0.2
-0.4
-0.6
-0.8
-0.4
0
0.4
0.8
T T
A T
A
C C
C
C
(C)
PC2
PC1
(B)
Gene CR Tg
Lipogenesis
Acc1
Acbd3
Acly
Acsl3
Acss2
Agpat6
Cyp51
Degs1
Dgat2
Dhcr24
Dhcr7
Ebp
Elovl5
Elovl6
Fads1
Far1
Fasn
Fdft1
Fdps
Gpam
Hmgcr
Hmgcs1
Hmgcs2
Hsd17b12
Hsd17b7
Idi1
LOC683884
LOC691221
Lss
Mecr
Mlycd
Mogat2
Mvd
Mvk
Nsdhl
Pc
Pecr
Pnpla3
Prkaa2
Prkab2
Ptgis
Sc4mol
Sc5dl
Scd
Scd1
Srebf1
Srebf2
Tecr
Ugcg
Gene CR Tg
Inflammatory
Acp5a
Aif1
Aldh1a2
Apoc3
Atrn
Bmp6
C1qbp
C4b
C5ar1
Ccl11
Ccl2
Ccl24
Ccl5
Ccl6
Ccl7
Ccl9
Ccne1
Ccr1
Ccr5
Cd14
Cd40
Cd44
Chst1
Col11a2
Col3a1
Coro1a
Crcp
Ctnnb1
Cxcl1
Cxcl13
Cxcl14
Cxcl16
Cxcl3
Cyba
Ddost
Ddt
Fcer1a
Fcer1g
Fcgr2a
Fcgrt
Fos
Ggt5
Ghr
Hdac7
Il6ra
Il6st
Itga1
Gene CR Tg
Inflammatory
Itgb2
Jun
Junb
Lipa
Mapk8
Mcl1
Mmp2
Mphosph8
Myd88
Nedd4
Nfkb2
Np
Orai1
Otub1
Oxtr
Pdgfra
Pdpn
Pecam1
Phb
Ppp3cb
Ptafr
Pum1
Pycard
RT1-S3
Rxra
S1pr3
Sdc1
Sels
Serpina3n
Sgms1
Slc37a4
Sparc
Sphk1
Spp1
Stat1
Stat6
Synj1
Tgfb1
Timp1
Timp2
Tlr2
Tlr4
Tnfrsf1a
Tollip
Trafd1
Vnn1
(D)
Gene CR Tg
SREBP-1 regulated
Acc1
Acly
Elovl5
Fasn
Sc5dl
Scd
Scd1
SREBP-2 regulated
Aacs
Acat2
Acly
Dhcr7
Fdps
Hes6
Hsd17b7
Idi1
Mvd
Mvk
Nsdhl
Sc4mol
Sc5dl
Sqle
decreased
increased
log10ratio -0.9
0
0.9

to compare the frequencies of genes matching specific categories or keywords in the GO Biological Process database; genes with $P<0.001$ are presented in Table 2. Among the 199 genes with PC1 >0.16, several were involved in metabolic processes, particularly lipid biosynthesis (GO 0008610, 0006633, and 0019432). Among the 226 genes with PC1 < –0.16, several genes were related to inflammation (GO 0006955, 0006954, 0034097, and 0030593).

To better define the effects of CR and Tg, the selected genes are indicated with yellow dots (GO 0008610, 0006633, and 0019432) and blue dots (GO 0006955, 0006954, 0034097, and 0030593) in the scatter plot (Fig. 2a), and are shown in a heat map (Fig. 2b). CR enhanced the expression of several genes involved in lipid biosynthesis (GO 0008610, 0006633, and 0019432) and suppressed the expression of genes involved in inflammation (GO 0006955, 0006954, 0034097, and 0030593). In contrast, Tg did not affect the expression of most of these genes. The effects of Tg appeared in PC2 as the groups located next to the axis; however, very few genes had large scores (Fig. 2a). In fact, we found no biological processes that were only affected by Tg (Table 2).

SREBPs are master transcriptional regulators of lipid metabolism and adipocyte differentiation. Three SREBP isoforms, 1a, 1c, and 2 have been identified (Osborne 2000; Osborne and Espenshade 2009). All three isoforms are synthesized as long inactive precursors, and SREBP cleavage-activating protein (SCAP) is required to convert these inactive precursors to transcriptionally active forms (Osborne 2000; Osborne and Espenshade 2009). Horton et al. identified and listed the genes regulated by SREBP-1 and SREBP-2 in vivo using transcriptome analysis of the liver of SREBP-1a transgenic, SREBP-2 transgenic, and SCAP knockout mice (Horton et al. 2003). We compared our data with theirs, and the SREBP-1- and SREBP-2-regulated genes are shown in a scatter plot with red and black dots, respectively (Fig. 2c). The SREBP-1- and SREBP-2-regulated genes identified by Horton et al. were observed in our heat map (Fig. 2d). SREBP-1-regulated genes were exclusively upregulated by CR, whereas SREBP-2-regulated genes were not, except for *ATP-citrate lyase* (*Acly*), which was also upregulated by SREBP-1 (Fig. 2c and d). Next, we examined the expression levels of *SREBP-1a*, *1c*, and *2*, and the genes regulated by SREBP-1 and SREBP-2 using real-time RT-PCR. We found that the expression of *SREBP*s was increased in WdCR, but not in TgAL, compared with WdAL. Among the *SREBP*s, it appears that CR had the strongest effect on *SREBP-1c* expression, followed by *SREBP-1a*, and the weakest effect on *SREBP-2* expression (Fig. 3a). The SREBP-1-regulated genes, *FASN* and *ACC1*, were upregulated in WdCR, but not in TgAL (Fig. 3b). In contrast, the SREBP-2-regulated genes, *Sqle* and *Mvk*, were not significantly upregulated in either WdCR or TgAL (Fig. 3c).

It is well-known that macrophages play a key role in inflammation in WAT of obese animals (Ouchi et al. 2011). An increased expression of MCP-1 [also known as chemokine (C-C motif) ligand 2] in WAT contributes to macrophage infiltration into WAT in obese mice (Kanda et al. 2006). Moreover, obesity leads to a shift from M2 (alternatively activated) macrophages to M1 (classically activated) macrophages in WAT (Lumeng et al. 2007). Therefore, we examined the expression of genes encoding the macrophage-specific transmembrane proteins, *F4/80*, *MCP-1*, the M1 macrophage-specific marker *CD11c* (also known as *integrin alpha X*), and the M2 macrophage-specific marker *CD163* (Kawanishi et al. 2010). As expected, the expression of *F4/80*, *MCP-1*, and *CD11c* was downregulated in WdCR, but not in TgAL, compared with WdAL. In contrast, CR and Tg did not significantly affect the expression of *CD163* (Fig. 3d).

◀ **Fig. 2** Principal component analysis of gene expression. **a** PC ordination of 6,641 ANOVA-positive genes based on the DNA microarray data of WdAL, WdCR, and TgAL (four biological repeats per group). *A*, *C*, and *T* represent WdAL, WdCR, and TgAL rats, respectively. The *yellow and blue dots* represent genes involved in lipid biosynthesis and inflammation, respectively. Gene function was defined based on annotations in the Gene Ontology (GO) Biological Process database (release 31) provided by the manufacturer. Genes involved in lipid biosynthesis were derived from the gene lists (GO: 0008610, 0006633, and 0019432). Genes involved in inflammation were derived from the gene lists (GO: 0006955, 0006954, 0034097, and 0030593). **b** Heat map of genes involved in lipid biosynthesis and inflammation. Genes involved in lipid biosynthesis were mostly upregulated by CR, while those involved in inflammation were predominantly downregulated by CR. The expression of these genes was not influenced by Tg. **c** Scatter plots of SREBP-1- (*red*) and SREBP-2- (*black*) regulated genes listed by Horton et al. (2003). All of the genes were included in the genes listed in GO 0008610, 0006633, and 0019432 (*yellow*). **d** Heat map of SREBP-1- and SREBP-2-regulated genes identified by Horton et al. (2003). Most of the SREBP-1-regulated genes were upregulated by CR, while most of the SREBP-2-regulated genes were not affected by CR

Table 2 List of ratios and *P* values of the selected GO terms

Gene ontology PC1>0	Biological process 199 genes selected	Ratio	*P* values
0008152	Metabolic process	37/756	7.9E-15
0055114	Oxidation reduction	23/591	8.2E-12
0008610	Lipid biosynthetic process	16/92	5.0E-14
0006629	Lipid metabolic process	13/232	5.2E-09
0006633	Fatty acid biosynthetic process	12/59	1.2E-14
0005975	Carbohydrate metabolic process	10/206	1.1E-06
0014070	Response to organic cyclic substance	9/274	8.1E-05
0008283	Cell proliferation	8/190	3.7E-05
0050873	Brown fat cell differentiation	7/34	3.5E-09
0006096	Glycolysis	7/45	2.3E-08
0016477	Cell migration	7/112	9.6E-06
0045471	Response to ethanol	7/153	6.8E-05
0010033	Response to organic substance	7/163	1.0E-04
0006090	Pyruvate metabolic process	6/21	6.9E-09
0009749	Response to glucose stimulus	6/118	1.3E-04
0006084	Acetyl-CoA metabolic process	5/11	1.3E-08
0019432	Triglyceride biosynthetic process	5/13	3.0E-08
0006641	Triglyceride metabolic process	5/40	7.1E-06
0005977	Glycogen metabolic process	5/42	9.0E-06
0006086	Acetyl-CoA biosynthetic process from pyruvate	4/7	1.6E-07
0009267	Cellular response to starvation	4/23	1.7E-05
0016126	Sterol biosynthetic process	4/28	3.6E-05
0006695	Cholesterol biosynthetic process	4/32	6.1E-05
0033574	Response to testosterone stimulus	4/41	1.6E-04
0009058	Biosynthetic process	4/58	5.8E-04
0042593	Glucose homeostasis	4/62	7.4E-04
0007595	Lactation	4/65	8.8E-04
PC1<0	226 genes selected		
0006955	Immune response	10/243	1.5E-05
0043066	Negative regulation of apoptosis	9/284	2.7E-04
0006954	Inflammatory response	7/170	2.8E-04
0030509	BMP signaling pathway	6/65	9.8E-06
0034097	Response to cytokine stimulus	6/119	2.7E-04
0030900	Forebrain development	5/94	6.9E-04
0009612	Response to mechanical stimulus	5/102	9.9E-04
0016525	Negative regulation of angiogenesis	4/29	6.8E-05
0030593	Neutrophil chemotaxis	4/35	1.4E-04
PC2>0	65 genes selected		
No annotation was significantly marked			
PC2<0	118 genes selected		
0051384	Response to glucocorticoid stimulus	5/163	4.3E-04
0048545	Response to steroid hormone stimulus	4/64	1.1E-04
0006006	Glucose metabolic process	4/79	2.6E-04

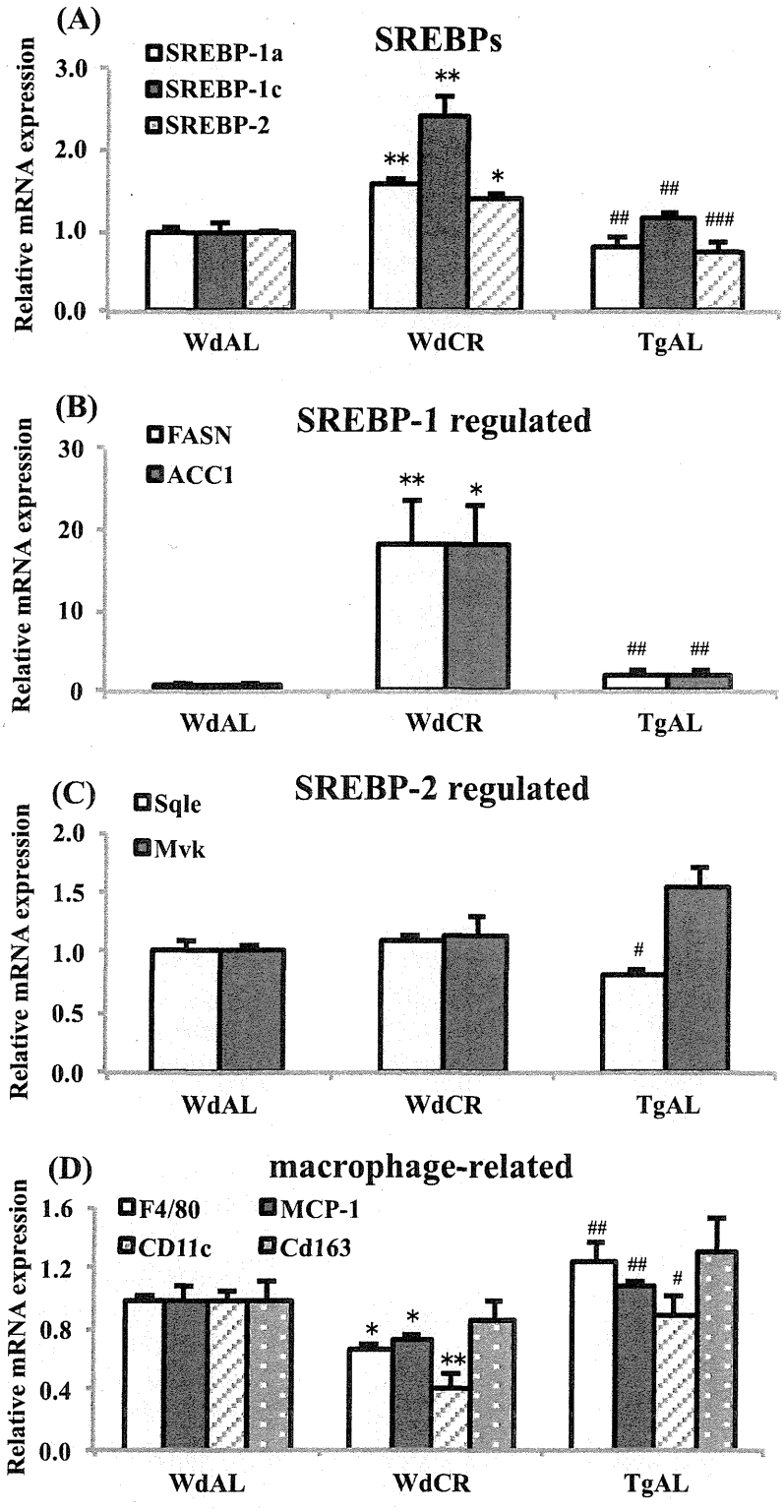

Fig. 3 Quantitative analysis of the mRNA expression of *SREBP*s, SREBP-1-regulated genes, SREBP-2-regulated genes, and macrophage-related genes in WdAL, WdCR, and TgAL rats. The mRNA expression levels in WAT of *SREBP*s (*A*: *SREBP-1a*, *SREBP-1c*, and *SREBP-2*), SREBP-1-regulated genes [*B*: *fatty acid synthase* (*FASN*) and *acyl CoA carboxylase 1* (*ACC1*)], SREBP-2-regulated genes [*C*: *squalene epoxidase* (*Sqle*) and *mevalonate kinase* (*Mvk*)], and macrophage-related genes [*D monocyte chemotactic protein-1* (*MCP-1*), *F4/80*, *integrin alpha X* (*Itgax*, *CD11c*), and *CD163*] were analyzed by real-time RT-PCR. Data were normalized against *TBP* expression. Values are means±SEM (n=3–6). *P<0.05, **P<0.01, and ***P<0.001 vs. WdAL; $^{\#}P$<0.05, $^{\#\#}P$<0.01, and $^{\#\#\#}P$<0.001 vs. WdCR (Tukey's t test)

To confirm the CR-associated SREBP-1- and macrophage-related gene expression profiles observed in wild-type rats, we analyzed the effect of CR on Tg rats. Similarly to the wild-type rats, CR markedly upregulated the expression of *SREBP-1c*, and slightly increased the expression of *SREBP-1a* (P=0.08; Fig. 4a). CR also markedly enhanced the expression of the SREBP-1-regulated genes, *FASN* and *ACC1*

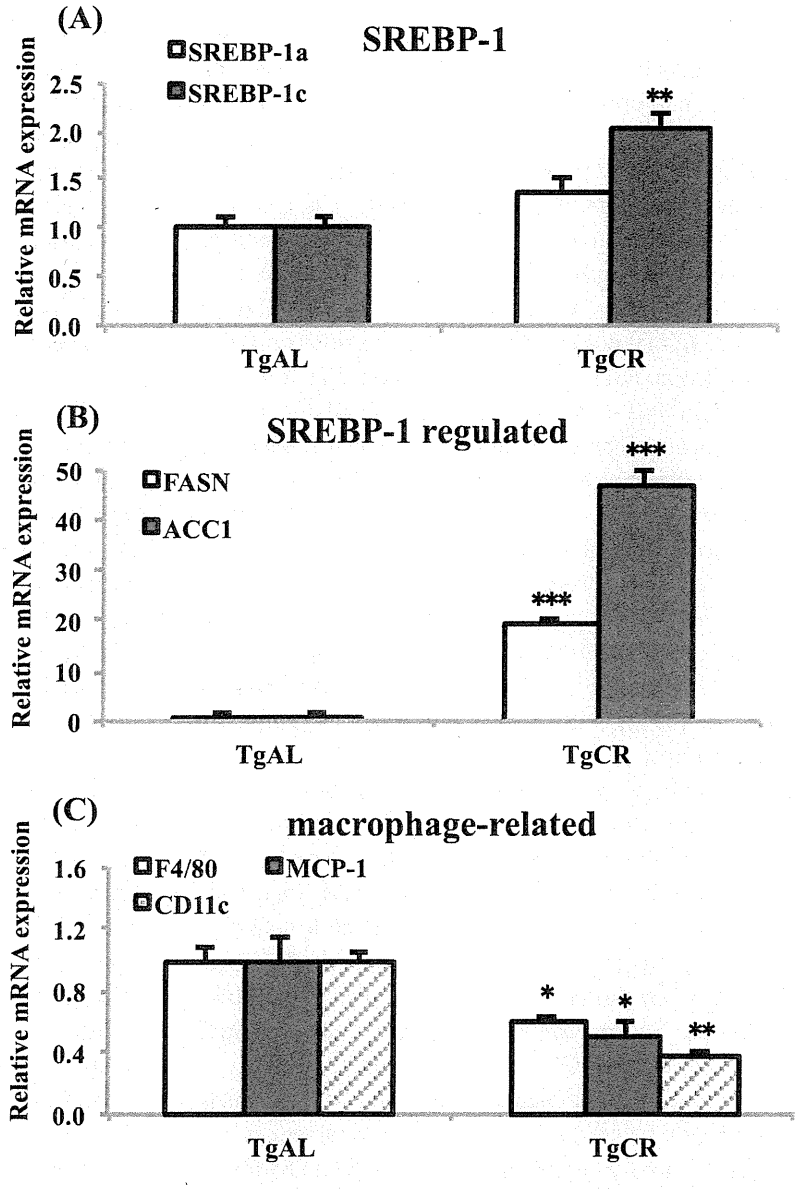

Fig. 4 Quantitative analysis of the mRNA expression of *SREBP*s, SREBP-1-regulated genes, and macrophage-related genes in TgAL and TgCR rats. The mRNA expression levels in WAT of *SREBP*s (**a** *SREBP-1a* and *SREBP-1c*), SREBP-1-regulated genes [**b** *fatty acid synthase* (*FASN*) and *acyl CoA carboxylase 1* (*ACC1*)], and macrophage-related genes [**c** *F4/80*, *monocyte chemotactic protein-1* (*MCP-1*), *integrin alpha X* (*Itgax*, *CD11c*)] were analyzed by real-time RT-PCR. Data were normalized against *TBP* expression. Values are means±SEM (n= 4–5). *P<0.05, **P<0.01, and ***P<0.001 vs. TgAL (Tukey's t test)

(Fig. 4b), while it significantly downregulated the expression of the macrophage-involved genes, *F4/80*, *MCP-1*, and *CD11c* in Tg rats (Fig. 4c).

Discussion

In the current study, we found that CR markedly reduced the size of adipocytes in WAT of wild-type rats (Fig. 1a, b, f, and g), but this CR effect was blunted in Tg rats (Fig. 1c, d, f, and g). Tg also significantly reduced adipocyte size, but this effect of Tg was less than that of CR (Fig. 1a, b, c, f, and g). When looking at adiposity (WAT weight as a percentage of body weight), the effect of CR was predominantly found in wild-type rats rather than Tg rats. It is well-known that small adipocytes secrete more adiponectin and less pro-inflammatory cytokines, including TNF-α and leptin, and are generally more sensitive to insulin (Ouchi et al. 2011). Moreover, small adipocytes act as powerful buffers by absorbing lipids in the postprandial period. If this buffering action is impaired, lipids in the form of TG accumulate in non-adipose tissues, resulting in insulin resistance (Frayn 2002). Recently, it has been reported that inflammatory cells preferentially infiltrate into WAT containing large adipocytes (Ouchi et al. 2011). Therefore, the CR-associated adipokine profile, the

inhibition of inflammatory cell infiltration, and the buffering activity in WAT may represent beneficial factors that contribute to the anti-aging and pro-longevity effects of CR. The plasma levels of IGF-1, insulin, adiponectin, and leptin in these rats have been reported elsewhere (Higami et al. 2006b; Yamaza et al. 2007). Briefly, the plasma IGF-1 and insulin concentrations were highest in WdAL rats, followed by WdCR rats, then TgAL, and lowest in TgCR rats, suggesting that plasma insulin concentrations correlate with plasma IGF-1 levels. In contrast, the levels of insulin and IGF-1 did not correlate with adipocyte size and adiposity. Therefore, adipocyte size and adiposity are not simply regulated in a GH–IGF-1- and/or insulin-dependent manner. Plasma adiponectin concentrations were higher in WdCR and TgAL rats than in WdAL rats. Plasma leptin concentrations were highest in WdAL rats, followed by TgAL rats, and lowest in WdCR rats. Because the plasma IGF-1 concentrations did not correlate with the plasma adiponectin or leptin concentrations among the three groups, it is likely that these parameters do not depend on IGF-1. However, continuous infusion of recombinant IGF-1 suppressed the CR-associated increase in plasma adiponectin levels (Yamaza et al. 2007). Moreover, CR and Tg equally enhanced glucose tolerance and insulin sensitivity (Yamaza et al. 2004). Therefore, the CR-associated adipokine profile, including adiponectin and leptin, and insulin sensitivity may be regulated, in part, in a GH–IGF-1-dependent manner.

Our transcriptome analysis combined with PC analysis revealed that CR upregulated several genes involved in lipid biosynthesis (GO 0008610, 0006633, and 0019432) and downregulated several genes associated with inflammation (GO 0006955, 0006954, 0034097, and 0030593; Fig. 2a and b and Table 2). These findings support our previous transcriptome analysis in mice (Higami et al. 2004, 2006a). We also found that CR was more effective than Tg in modulating these genes. Our data also demonstrated that the CR-associated changes in the expression of genes involved in lipid biosynthesis and inflammation occurred in a GH–IGF-1-independent manner (Fig. 2a and b).

Previously, we reported that in the liver of both wild-type and Tg rats, with the same background used in the present study, CR induced the expression of genes involved in fatty acid biosynthesis, probably via SREBP-1 (Higami et al. 2006b). SREBPs, transcription factors belonging to the basic helix-loop-helix-leucine zipper family, are master regulators of lipid metabolism and adipocyte differentiation. The three SREBP isoforms (1a, 1c, and 2) are expressed at varying levels in different tissues and act as homo- and hetero-dimers to activate gene expression (Osborne 2000; Osborne and Espenshade 2009). All three SREBPs are synthesized as long inactive precursors. They are bound to membranes of the endoplasmic reticulum (ER), where the C-terminal regulatory domain of SREBPs interacts with SCAP (Osborne and Espenshade 2009). SCAP escorts SREBPs from the ER to the Golgi apparatus, where they are cleaved sequentially by site-1 and site-2 proteases, to yield the active proteins. The active SREBPs consist of an NH_2-terminal domain and can enter the nucleus to activate transcription (Osborne and Espenshade 2009). SREBP-1a and SREBP-1c are encoded by a single gene and are transcribed by alternate promoters. They stimulate the expression of genes that are preferentially involved in fatty acid and triglyceride biosynthesis. In contrast, SREBP-2 is encoded by a different gene and induces the expression of genes predominantly involved in cholesterol biosynthesis (Osborne 2000; Osborne and Espenshade 2009). When we compared our data with the SREBP-1- and SREBP-2-regulated genes listed by Horton et al. (2003), we found that in wild-type rats SREBP-1-regulated genes were exclusively upregulated by CR, whereas SREBP-2-regulated genes were not (Fig. 2c and d). Subsequent real-time RT-PCR analysis confirmed that CR, but not Tg, upregulated the expression of the SREBP-1-regulated genes, *FASN* and *ACC1*. In contrast, CR and Tg did not upregulate the SREBP-2-regulated genes, *Sqle* and *Mvk* (Fig. 3). The CR effect on the expression of *SREBP-1* and the regulated genes was further confirmed in Tg rats (Fig. 4a and b). Therefore, we concluded that CR preferentially enhances the expression of SREBP-1-regulated genes, but not SREBP-2-regulated genes, in a GH–IGF-1-independent manner.

As described above, inflammatory cells, particularly macrophages, preferentially infiltrate into the WAT of obese animals (Ouchi et al. 2011). The majority of previous studies have examined F4/80 expression as a marker to identify adipose tissue-specific macrophages (Lumeng et al. 2007). MCP-1, which shows increased expression in WAT of obese animals, promotes adipose tissue inflammation and macrophage recruitment (Kanda et al. 2006). Therefore, we measured the expression of genes encoding *F4/80* and *MCP-1* in wild-type and Tg rats (Figs. 3d and 4c). We found that CR, but not

Tg, reduced the expressions of *F4/80* and *MCP-1*, suggesting that CR suppresses macrophage infiltration by decreasing the expression of *MCP-1* in a GH–IGF-1-independent manner. Lumeng et al. (2007) reported that the $F4/80^{+}CD11c^{+}$ population of macrophages, a characteristic of M1 macrophages, was present in WAT of obese mice, but not in lean mice. In contrast, the macrophages in WAT of lean mice expressed many genes characteristic of M2 macrophages. Thus, obesity leads to a shift in the activation state of macrophages in WAT from an M2-polarized state in lean animals that may protect adipocytes from inflammation to an M1 pro-inflammatory state that contributes to insulin resistance (Lumeng et al. 2007). Unlike WAT in obese animals, our data suggest that the reduced infiltration of macrophages is mainly due to the decreased shift towards $F4/80^{+}CD11c^{+}$ M1 macrophages in WAT of both wild-type and Tg CR rats.

In this study, we demonstrated that CR-associated morphological changes preferentially found in WAT of wild-type rats rather than Tg rats are not solely regulated in a GH–IGF-1-dependent manner. Moreover, CR-enhanced lipid biosynthesis and CR-suppressed inflammation were only regulated in a GH–IGF-1-independent manner. In particular, CR-associated activation of lipid biosynthesis was predominantly regulated by SREBP-1. Recently, it has been hypothesized that CR-associated lipid utilization may reduce reactive oxygen species production (Guarente 2008). In fact, SREBP-1-regulated de novo lipid biosynthesis in WAT may play an important role in CR-associated lipid utilization (Okita et al. 2012). In addition, it has been reported that molecular inflammation, which is associated with nuclear factor-κB activation and enhanced expression of several pro-inflammatory cytokines, is involved in the aging process and is attenuated by CR (Chung et al. 2011). Therefore, we suggest that the activation of de novo lipid biosynthesis by SREBP-1 and the induction of anti-inflammatory conditions by reduced macrophage infiltration are pivotal regulators of CR-associated WAT remodeling, and may be important factors in the beneficial effects of CR.

Acknowledgments We thank Yutaka Araki and Yuko Moriyama (Department of Investigative Pathology, Nagasaki University Graduate School for Biomedical Sciences) for their technical assistance and cooperation. This work was supported by a Grant-in-Aid for Scientific Research (C) from the Japan Society for the Promotion of Science (no. 19590396).

References

Al-Regaiey KA, Masternak MM, Bonkowski M, Sun L, Bartke A (2005) Long-lived growth hormone receptor knockout mice: interaction of reduced insulin-like growth factor I/insulin signaling and caloric restriction. Endocrinology 146:851–860

Anderson R, Prolla T (2009) PGC-1alpha in aging and anti-aging interventions. Biochem Biophys Acta 1790:1059–1066

Argmann C, Dobrin R, Heikkinen S, Auburtin A, Pouilly L, Cock TA, Koutnikova H, Zhu J, Schadt EE, Auwerx J (2009) Ppargamma2 is a key driver of longevity in the mouse. PLoS Genet 5:e1000752

Bartke A (2005) Minireview: role of the growth hormone/insulin-like growth factor system in mammalian aging. Endocrinology 146:3718–3723

Bartke A, Wright JC, Mattison JA, Ingram DK, Miller RA, Roth GS (2001) Extending the lifespan of long-lived mice. Nature 414:412

Barzilai N, Banerjee S, Hawkins M, Chen W, Rossetti L (1998) Caloric restriction reverses hepatic insulin resistance in aging rats by decreasing visceral fat. J Clin Invest 101:1353–1361

Blüher M, Michael MD, Peroni OD, Ueki K, Carter N, Kahn BB, Kahn CR (2002) Adipose tissue selective insulin receptor knockout protects against obesity and obesity-related glucose intolerance. Dev Cell 3:25–38

Blüher M, Kahn BB, Kahn CR (2003) Extended longevity in mice lacking the insulin receptor in adipose tissue. Science 299:572–574

Bonkowski MS, Rocha JS, Masternak MM, Al Regaiey KA, Bartke A (2006) Targeted disruption of growth hormone receptor interferes with the beneficial actions of calorie restriction. Proc Natl Acad Sci U S A 103:7901–7905

Brown-Borg HM, Borg KE, Mellska CJ, Bartke A (1996) Dwarf mice and the ageing process. Nature 384:33

Chiu CH, Lin WD, Huang SY, Lee YH (2004) Effect of a C/EBP gene replacement on mitochondrial biogenesis in fat cells. Genes Dev 18:1970–1975

Chung HY, Lee EK, Choi YJ, Kim JM, Kim DH, Zou Y, Kim CH, Lee J, Kim HS, Kim ND, Jung JH, Yu BP (2011) Molecular inflammation as an underlying mechanism of the aging process and age-related diseases. J Dent Res 90:830–840

Coschigano KT, Clemmons D, Bellush LL, Kopchick JJ (2000) Assessment of growth parameters and life span of GHR/BP gene-disrupted mice. Endocrinology 141:2608–2613

Farmer SR (2006) Transcriptional control of adipocyte formation. Cell Metab 4:263–273

Flurkey K, Papaconstantinou J, Miller RA, Harrison DE (2001) Lifespan extension and delayed immune and collagen aging in mutant mice with defects in growth hormone production. Proc Natl Acad Sci U S A 98:6736–6741

Frayn KN (2002) Adipose tissue as a buffer for daily lipid flux. Diabetologia 45:1201–1210

Gesing A, Masternak MM, Wang F, Joseph AM, Leeuwenburgh C, Westbrook R, Lewinski A, Karbownik-Lewinska M, Bartke A (2011) Expression of key regulators of mitochondrial biogenesis in growth hormone receptor knockout

(GHRKO) mice is enhanced but is not further improved by other potential life-extending interventions. J Gerontol A Biol Sci Med Sci 66:1062–1076

Guarente L (2008) Mitochondria—a nexus for aging, calorie restriction, and sirtuins? Cell 132:171–176

Hancock CR, Han DH, Higashida K, Kim SH, Holloszy JO (2011) Does calorie restriction induce mitochondrial biogenesis? A reevaluation. FASEB J 25:785–791

Higami Y, Pugh TD, Page GP, Allison DB, Prolla TA, Weindruch R (2004) Adipose tissue energy metabolism: altered gene expression profile of mice subjected to long-term caloric restriction. FASEB J 18:415–417

Higami Y, Yamaza H, Shimokawa I (2005) Laboratory findings of caloric restriction in rodents and primates. Adv Clin Chem 39:211–237

Higami Y, Barger JL, Page GP, Allison DB, Smith SR, Prolla TA, Weindruch R (2006a) Energy restriction lowers the expression of genes linked to inflammation, the cytoskeleton, the extracellular matrix, and angiogenesis in mouse adipose tissue. J Nutr 136:343–352

Higami Y, Tsuchiya T, Chiba T, Yamaza H, Muraoka I, Hirose M, Komatsu T, Shimokawa I (2006b) Hepatic gene expression profile of lipid metabolism in rats: impact of caloric restriction and growth hormone/insulin-like growth factor-1 suppression. J Gerontol A Biol Sci Med Sci 61:1099–1110

Holzenberger M, Dupont J, Ducos B, Leneuve P, Géloën A, Even PC, Cervera P, Le Bouc Y (2003) IGF-1 receptor regulates lifespan and resistance to oxidative stress in mice. Nature 421:182–187

Horton JD, Shah NA, Warrington JA, Anderson NN, Park SW, Brown MS, Goldstein JL (2003) Combined analysis of oligonucleotide microarray data from transgenic and knockout mice identifies direct SREBP target genes. Proc Natl Acad Sci U S A 100:12027–12032

Jackson JE (2005) A user's guide to principal components. Wiley, New York

Kanda H, Tateya S, Tamori Y, Kotani K, Hiasa K, Kitazawa R, Kitazawa S, Miyachi H, Maeda S, Egashira K, Kasuga M (2006) MCP-1 contributes to macrophage infiltration into adipose tissue, insulin resistance, and hepatic steatosis in obesity. J Clin Invest 116:1494–1505

Kawanishi N, Yano H, Yokogawa Y, Suzuki K (2010) Exercise training inhibits inflammation in adipose tissue via both suppression of macrophage infiltration and acceleration of phenotypic switching from M1 to M2 macrophages in high-fat-diet-induced obese mice. Exerc Immunol Rev 16:105–118

Konishi T, Konishi F, Takasaki S, Inoue K, Nakayama K, Konagaya A (2008) Coincidence between transcriptome analyses on different microarray platforms using a parametric framework. PLoS One 3:e3555

Koo H-Y, Miyashita M, Cho BH, Nakamura MT (2009) Replacing dietary glucose with fructose increases ChREBP activity and SREBP-1 protein in rat liver nucleus. Biochem Biophys Res Commun 390:285–289

López-Lluch G, Hunt N, Jones B, Zhu M, Jamieson H, Hilmer S, Cascajo MV, Allard J, Ingram DK, Navas P, de Cabo R (2006) Calorie restriction induces mitochondrial biogenesis and bioenergetic efficiency. Proc Natl Acad Sci USA 103:1768–1773

Lumeng CN, Bodzin JL, Saltiel AR (2007) Obesity induces a phenotypic switch in adipose tissue macrophage polarization. J Clin Invest 117:175–184

Masoro EJ (2005) Overview of caloric restriction and ageing. Mech Ageing Dev 126:913–922

Masternak MM, Bartke A, Wang F, Spong A, Gesing A, Fang Y, Salmon AB, Hughes LF, Liberati T, Boparai R, Kopchick JJ, Westbrook R (2012) Metabolic effects of intra-abdominal fat in GHRKO mice. Aging Cell 11:73–81

Nisoli E, Tonello C, Cardile A, Cozzi V, Bracale R, Tedesco L, Falcone S, Valerio A, Cantoni O, Clementi E, Moncada S, Carruba MO (2005) Calorie restriction promotes mitochondrial biogenesis by inducing the expression of eNOS. Science 310:314–317

Okita N, Hayashida Y, Kojima Y, Fukushima M, Yuguchi K, Mikami K, Yamauchi A, Watanabe K, Noguchi M, Nakamura M, Toda T, Higami Y (2012) Differential responses of white adipose tissue and brown adipose tissue to caloric restriction in rats. Mech Ageing Dev 133:255–266

Osborne TF (2000) Sterol regulatory element-binding proteins (SREBPs): key regulators of nutritional homeostasis and insulin action. J Biol Chem 275:32379–32382

Osborne TF, Espenshade PJ (2009) Evolutionary conservation and adaptation in the mechanism that regulates SREBP action: what a long, strange tRIP it's been. Genes Dev 23:2578–2591

Otabe S, Yuan X, Fukutani T, Wada N, Hashinaga T, Nakayama H, Hirota N, Kojima M, Yamada K (2007) Overexpression of human adiponectin in transgenic mice results in suppression of fat accumulation and prevention of premature death by high-calorie diet. Am J Physiol Endocrinol Metab 293:E210–E218

Ouchi N, Parker JL, Lugus JJ, Walsh K (2011) Adipokines in inflammation and metabolic disease. Nat Rev Immunol 11:85–97

Saely CH, Geiger K, Drexel H (2012) Brown versus white adipose tissue: a mini-review. Gerontology 58:15–23

Shi T, Wang F, Stieren E, Tong Q (2005) SIRT3, a mitochondrial sirtuin deacetylase, regulates mitochondrial function and thermogenesis in brown adipocytes. J Biol Chem 280:13560–13567

Shimokawa I, Higami Y, Utsuyama M, Tuchiya T, Komatsu T, Chiba T, Yamaza H (2002) Life span extension by reduction in growth hormone-insulin-like growth factor-1 axis in a transgenic rat model. Am J Pathol 160:2259–2265

Shimokawa I, Higami Y, Tsuchiya T, Otani H, Komatsu T, Chiba T, Yamaza H (2003) Life span extension by reduction of the growth hormone-insulin-like growth factor-1 axis: relation to caloric restriction. FASEB J 17:1108–1109

Sinclair DA (2005) Toward a unified theory of caloric restriction and longevity regulation. Mech Ageing Dev 126:987–1002

Sohal RS, Weindruch R (1996) Oxidative stress, caloric restriction, and aging. Science 273:59–63

Torres-Leal FL, Fonseca-Alaniz MH, Rogero MM, Tirapegui J (2010) The role of inflamed adipose tissue in the insulin resistance. Cell Biochem Funct 28:623–631

Weindruch R, Walford RL (1988) The retardation of aging and disease by dietary restriction. Charles C Thomas, Springfield

Yamaza H, Komatsu T, Chiba T, Toyama H, To K, Higami Y, Shimokawa I (2004) A transgenic dwarf rat model as a tool

for the study of calorie restriction and aging. Exp Gerontol 39:269–272

Yamaza H, Komatsu T, To K, Toyama H, Chiba T, Higami Y, Shimokawa I (2007) Involvement of insulin-like growth factor-1 in the effect of caloric restriction: regulation of plasma adiponectin and leptin. J Gerontol A Biol Sci Med Sci 62:27–33

Yang J, Goldstein JL, Hammer RE, Moon YA, Brown MS, Horton JD (2001) Decreased lipid synthesis in livers of mice with disrupted site-1 protease gene. Proc Natl Acad Sci 98:13607–13612

Yu BP (1994) Modulation of aging processes by dietary restriction. CRC, Boca Raton

Biochemical and Biophysical Research Communications 427 (2012) 758–763

Contents lists available at SciVerse ScienceDirect

Biochemical and Biophysical Research Communications

journal homepage: www.elsevier.com/locate/ybbrc

Autophagosomes accumulate in differentiated and hypertrophic adipocytes in a p53-independent manner

Kentaro Mikami, Naoyuki Okita, Yuki Tokunaga, Tomoyo Ichikawa, Tatsuya Okazaki, Kanako Takemoto, Wataru Nagai, Shingo Matsushima, Yoshikazu Higami *

Molecular Pathology & Metabolic Disease, Faculty of Pharmaceutical Sciences, Tokyo University of Science, Tokyo, Japan

ARTICLE INFO

Article history:
Received 25 September 2012
Available online 4 October 2012

Keywords:
p53
Adipocyte
Differentiation
Obesity
Autophagosome
Autophagic flux

ABSTRACT

Autophagy is induced by several kinds of stress, including oxidative, genotoxic, endoplasmic reticulum and nutrient stresses. The tumor suppressor p53, which is a stress sensor, plays a critical role in the regulation of autophagy. Although p53 is required for starvation (nutrient deficient stress)-induced autophagy, it is still not clear whether p53 is also required for the autophagy observed in differentiated and hypertrophic adipocytes, which accumulate excessive amounts of nutrients in the form of triglycerides. In this study, we demonstrated that starvation induces autophagy in p53-proficient adipocytes, but not in p53-deficient adipocytes as previously reported. On the other hand, autophagy was equally observed in both p53-deficient and -proficient differentiated and hypertrophic adipocytes. Similar results were obtained by *in vivo* analysis using white adipose tissue of high-fat diet-induced obese mice. Moreover, unexpectedly, the autophagy observed in the differentiated and hypertrophic adipocytes involved increased accumulation of autophagosomes and decreased autophagic flux. Thus, we concluded that in differentiated and hypertrophic adipocytes autophagosomes accumulate in a p53-independent manner, and this accumulation is caused by reduced autophagic flux.

© 2012 Elsevier Inc. All rights reserved.

1. Introduction

Autophagy is a major cytosolic catabolic process operating through the lysosomal machinery, and playing an important role in cellular and/or organism homeostasis against diverse pathologies [1–4]. In this process, autophagy is initiated by autophagosome formation, surrounding cytoplasmic components with a double-membrane. Then, the autophagosome fuses with a lysosome to form an autolysosome and subsequently degrades the intramembrane contents. During autophagosome formation, microtubule-associated protein 1–light chain 3 (LC3) is lipidated, converting LC3-I (non-lipidated form) to LC3-II (lipidated form). Autophagy is the key machinery for the turnover of cellular components and/or proteins including p62, which seems to be a selective substrate for autophagy [2–4]. Therefore, the conversion of LC3-I to LC3-II, the aggregation of LC3-II and the degradation of p62 are hallmarks of the autophagic process [2–4].

The tumor suppressor p53 is involved in several cellular stress responses [5]. Recently, it has been reported that p53 plays a critical role in the autophagic process and metabolic process [6–10]. p53 promotes autophagy through inhibition of mammalian target of rapamycin (mTOR) [8]. p53 also transcriptionally promotes the expression of autophagy-regulated genes such as Sestrin2 and DRAM [9,10].

Previously, it has been reported that autophagic vacuoles are frequently found in differentiated and hypertrophic 3T3-L1 adipocytes [11]. Furthermore, targeted deletion of atg5 or atg7, which are necessary for the autophagic process, interferes with normal adipocyte differentiation, suggesting that autophagy regulates adipocyte differentiation and/or lipid accumulation [12–15]. Moreover, inhibition of autophagy increases triglyceride storage in lipid droplets in cultured hepatocytes and mouse liver [16]. Thus, these studies indicate that autophagy is involved in adipogenesis and lipid metabolism.

In the present study, to understand the molecular basis of autophagy observed in differentiated and hypertrophic adipocytes, we investigated whether p53 is required for autophagy in differentiated and hypertrophic adipocytes associated with excessive nutrient accumulation using both *in vitro* and *in vivo* models. Moreover, we evaluated whether the autophagic machinery is fully activated in differentiated and hypertrophic adipocytes *in vitro*.

2. Materials and methods

2.1. Animals

Experiments on mice were conducted in accordance with the provisions of the Ethics Review Committee for Animal

* Corresponding author. Address: Molecular Pathology & Metabolic Disease, Faculty of Pharmaceutical Sciences, Tokyo University of Science, 2641 Yamazaki, Noda, Chiba 278-8510, Japan. Fax: +81 4 7121 3676.
E-mail address: higami@rs.noda.tus.ac.jp (Y. Higami).

0006-291X/$ - see front matter © 2012 Elsevier Inc. All rights reserved.
http://dx.doi.org/10.1016/j.bbrc.2012.09.134

Experimentation at Tokyo University of Science. p53 heterozygous knockout ($p53^{+/-}$) mice with C57BL/6J background (Accession Number, CDB0001K) were purchased from RIKENBRC (Saitama, Japan). These mice were intercrossed to obtain wild-type ($p53^{+/+}$) and homozygous knockout ($p53^{-/-}$) mice. Male $p53^{+/+}$ and $p53^{-/-}$ mice were weaned four weeks after birth. Mice were housed in a temperature-controlled environment with a 12-h light/dark cycle and free access to water and a normal-fat diet (NFD; NOSAN, Kanagawa, Japan) or high-fat diet (HFD; CREA, Tokyo, Japan) for nine weeks. Mice were sacrificed at 13 weeks of age and the epididymal white adipose tissue (WAT) was collected.

2.2. Cell lines and reagents

The p53-proficient preadipocyte cell line, 3T3-L1, was purchased from RIKENBRC. The p53-deficient preadipocyte cell line, HW, was kindly provided by Dr. Masayuki Saito (Tenshi University, Japan). Primary mouse embryonic fibroblasts (MEFs) derived from wildtype ($p53^{+/+}$) and p53-knockout ($p53^{-/-}$) mice were established as previously described [17].

Etoposide and camptothecin were purchased from WAKO (Osaka, Japan). Rapamycin and bafilomycin A1 were purchased from LC Laboratories (Woburn, MA, USA).

2.3. Vector construction

The pMXs-puro (-U3) –Cul2 and pMXs-puro (-U3) Kpc1 vectors were kindly gifted by Dr. Takumi Kamura (Nagoya University, Japan). To construct the backbone vector, pMXs-puro-mU6 [18], the mouse U6 gene promoter was obtained from the pMXs-puro (-U3) Kpc1 vector by PCR, using the following primers: forward – 5′-GGCAAAACTCGAGTTCGAACGCGTGATCAATTGTTTAAACAAGGCT TTTCTCCAGGGATATTTATAGTA-3′, and reverse – 5′-GTCGAC-CACTGTGCTGGC-3′. The PCR product was digested with NotI/XhoI and subcloned into the NotI/XhoI sites of the pMXs-puro (-U3) – Cul2 vector, yielding the pMXs-puro-mU6 shRNA vector. We designed a mouse p53 shRNA expression vector based on target sequences for effective p53 knockdown as previously reported [19]. The oligonucleotides for shp53 and the shGFP control were chemically synthesized (Operon Biotechnology, Tokyo, Japan) as follows. shp53-1: 5′-GTACGTGTGTAGTAGCTTCttcaagagaGGAGC-TATTACACATGTACttttt-3′ and 5′-cgaaaaaGTACATGTGTAATAGCTCC tctcttgaaGAAGCTACTACACACGTAC-3′; shp53-2: 5′-GGAGTAGGTT GGTAGTTGTTATTCAAGAGATGACAACTATCAACCTATTCCCCttttt-3′ and 5′-cgaaaaaGGGGAATAGGTTGATAGTTGTCATCTCTTGAATA ACAACTACCAACCTACTCC-3′; shGFP: 5′-GGCTATGTCCAGGGGCG-CATCttcaagagaGGTGCGCTCCTGGACGTAGCCttttt-3′ and 5′-cgaaaaa GGCTACGTCCAGGAGCGCACCtctcttgaaGATGCGCCCCTGGACATAGC C-3′ (upper case letters, target sequences against p53 or GFP; lower case letters, BstBI or loop structure sequences). The annealed oligos were directly ligated into a PmeI and BstBI-digested pMXs-puro-mU6 shRNA expression vector.

2.4. Establishment of stable p53-knockdown 3T3-L1 preadipocytes

Stable p53-knockdown cell lines were generated using retroviral infection as previously reported [20]. The produced vectors, termed pMXs-puro-mU6-shp53 or shGFP, were transfected into Plat-E cells with FuGENE®6 (Promega, Madison, WI, USA), according to the manufacturer's protocol. Virus-containing culture supernatants were collected 2 d after the transfection and filtered through 0.22-μm filters (Millipore, Billerica, MA, USA). To obtain stable p53- or GFP-knockdown cell lines (3T3-L1/shp53 or 3T3-L1/shGFP), 3T3-L1 cells were incubated with virus-containing medium for 2 d, followed by selection with 2 μg/mL puromycin for 5 d.

2.5. Cell culture and treatments

Preadipocyte cell lines were maintained in maintenance medium. Preadipocyte cell lines were differentiated as previously described [21]. In brief, cells were seeded to reach confluency after 2 d. At confluence, the maintenance medium was changed to adipocyte differentiation medium (AD medium), and the cells were cultured for another 2 d. For adipocyte maturation, the differentiation-induced cells were grown in adipocyte maturation medium (AM medium), which was changed every other day. The maintenance medium contained 10% FBS (Sigma, Saint Louis, MO, USA) and 1% penicillin/streptomycin (Sigma) in DMEM low glucose (WAKO). AD medium contained 500 μM 3-isobutyl-1-methylxanthine (Sigma) and 1 μM dexamethasone (Sigma) in maintenance medium, and AM medium contained 10 μg/mL insulin (Sigma) and 50 nM tri-iode thyronine (T3; Sigma) in maintenance medium.

To induce adipocyte differentiation in MEFs, MEFs were seeded to reach confluence. At confluence, the maintenance medium was changed to MEF differentiation medium, which contained 500 μM 3-isobutyl-1-methylxanthine, 1 μM dexamethasone, 10 μg/mL insulin and 100 μM troglitazone (WAKO). The medium was changed to fresh MEF differentiation medium every other day.

To induce nutrient starvation, the maintenance medium was changed to DMEM without FBS (serum-free) followed by incubation for 24 h. To induce autophagy via inhibition of mTOR, cells were treated with 500 nM rapamycin for 6 h.

To analyze autophagic flux, adipocytes were differentiated for 3 or 11 d, followed by a medium change with fresh AM medium containing 10 nM bafilomycin A1 (Baf; LC Laboratories) for a 24-h incubation.

2.6. Western blot

Western blot analysis was performed as previously described [17] with the following primary antibodies: LC3 (PM036, MBL, Nagoya, Japan), p62 (PM045, MBL), p53 (PO03, MBL), β-actin (A1978, Sigma) and α-tubulin (T6199, Calbiochem, Darmstadt, Germany). The secondary antibodies used were: horseradish peroxidase-conjugated $F(ab')_2$ fragment of goat anti-mouse IgG or anti-rabbit IgG (Jackson Immunoresearch, West Grove, PA, USA).

2.7. Oil Red O staining

Cells were fixed with 10% neutral-buffered formalin. Fixed cells were washed with 60% isopropanol and stained with 60% isopropanol containing 0.18% Oil Red O for 20 min. Stained cells were washed with 60% isopropanol for 1 min. Images were captured by a BIOREVO BZ9000 fluorescence microscope (KEYENCE, Osaka, Japan).

2.8. Immunocytochemistry and confocal laser microscopy

Cells were seeded on poly-D-lysine-coated coverslips. For LC3 immunocytochemistry, cells were fixed in 4% paraformaldehyde and permeabilized with PBS containing 0.2% Triton-X 100 for 10 min. After washing with PBS containing 0.1% Tween 20 (TPBS), cells were blocked in TPBS containing 2% BSA and 5% goat serum. Following washes with TPBS, cells were incubated with LC3 antibodies in a moist chamber overnight at 4 °C. Next, cells were washed with TPBS and probed with the secondary antibody, Alexa Fluor 488-conjugated $F(ab')_2$ fragment of goat anti-rabbit IgG (Invitrogen, Carlsbad, CA, USA), for 30 min at room temperature. Confocal fluorescence images were captured using an LSM5Pascal Exciter laser-scanning microscope (Zeiss, Oberkochen, Germany).

2.9. Transmission electron microscopy analysis

Differentiated adipocytes were fixed with 2.5% gluteraldehyde in 0.2 M cacodylate buffer for 60 min, followed by incubation with 1% osmium tetroxide for 30 min. The samples were embedded in Epon. Selected areas were then sectioned with a Sorvall ultramicrotome MT-2 (Leica Mikrosystem GmbH, Vienna, Austria). Sections were observed under a JEM 1200EX II electron microscope (JEOL LTD, Tokyo, Japan) at 90 kV accelerating voltage.

2.10. Statistical analysis

Statistical analysis was performed by Tukey–Kramer test or Student's *t*-test (comparison of two means). The data are presented as mean ± standard deviation (S.D.). A *p*-value of less than 0.05 was considered significant.

3. Results

3.1. p53 is required for starvation-induced autophagy in 3T3-L1 and HW adipocytes

Treatment with the topoisomerase II inhibitor, etoposide, activated p53 in 3T3-L1 ($p53^{+/+}$) preadipocytes, but not in HW ($p53^{-/-}$) preadipocytes (Fig. 1A). mTOR plays a central role in the regulation of autophagy, and rapamycin induces autophagy via inhibition of mTOR [22]. In both 3T3-L1 and HW cells, 4 d after the induction of differentiation (day 4 adipocytes) rapamycin induced the conversion of LC3-I to LC3-II (Fig. 1B and C). In contrast, nutrient starvation (serum-free) induced the LC3 conversion and p62 degradation in day 4 3T3-L1 adipocytes, but not in day 4 HW adipocytes (Fig. 1D and E). Using confocal fluorescence microscopy analysis we observed that rapamycin treatment markedly increased LC3-positive puncta in both day 4 3T3-L1 and HW adipocytes. In contrast, after nutrient starvation LC3-positive puncta were increased in 3T3-L1 adipocytes but not in HW adipocytes (Fig. 1F). In agreement with previous reports [9,23], these findings suggest that p53 is necessary for starvation-induced autophagy in adipocytes.

3.2. p53 does not influence autophagy observed in differentiated and hypertrophic adipocytes

Oil Red O staining showed that 3T3-L1 and HW adipocytes accumulated TG (triglyceride) during adipocyte differentiation (Fig. 2A). Next, we investigated whether p53 participates in autophagy found at the late stage of adipocyte differentiation. The expression level of LC3-II in day 4 3T3-L1 and HW adipocytes was markedly suppressed compared with 3T3-L1 and HW preadipocytes, probably due to the medium change to insulin and tri-iode thyronine (T3) containing medium. The expression level of LC3-II in both 3T3-L1 and HW cells was similarly and significantly increased at the late stage of adipocyte differentiation (day 12 hypertrophic adipocytes) compared with day 4 adipocytes (Fig. 2B and C). In addition, LC3-positive puncta were found in both day 12 hypertrophic 3T3-L1 and HW adipocytes (Fig. 2D). Using electron microscopy several autophagosomes were observed in both day 12 hypertrophic adipocytes (Fig. 2E). These findings suggest that autophagy might be activated in differentiated and hypertrophic adipocytes in a p53-independent manner.

To confirm that the autophagy found in differentiated and hypertrophic adipocytes is p53-independent, we established stable shp53 3T3-L1 preadipocytes (3T3-L1/shp53). In 3T3-L1/shp53 preadipocytes, the camptothecin-induced p53 activation was markedly suppressed compared with 3T3-L1/shGFP preadipocytes (Fig. 3A). The expression of LC3-II and p62 was similarly increased during adipocyte differentiation in both 3T3-L1/shGFP and 3T3-L1/shp53 adipocytes (Fig. 3B). To further examine whether the autophagy observed in differentiated and hypertrophic adipocytes is p53-independent, primary mouse embryonic fibroblasts (MEFs) derived from wild type ($p53^{+/+}$) and p53-knockout ($p53^{-/-}$) mice were established. Oil Red O staining showed that both MEFs accumulated TG similarly after the induction of adipocyte differentiation for 20 d (Fig. 3C). Furthermore, the conversion of LC3-I to LC3-II was equally enhanced with the increased TG accumulation (Fig. 3D). These findings suggest that p53 does not influence the autophagic machinery observed in differentiated and hypertrophic adipocytes.

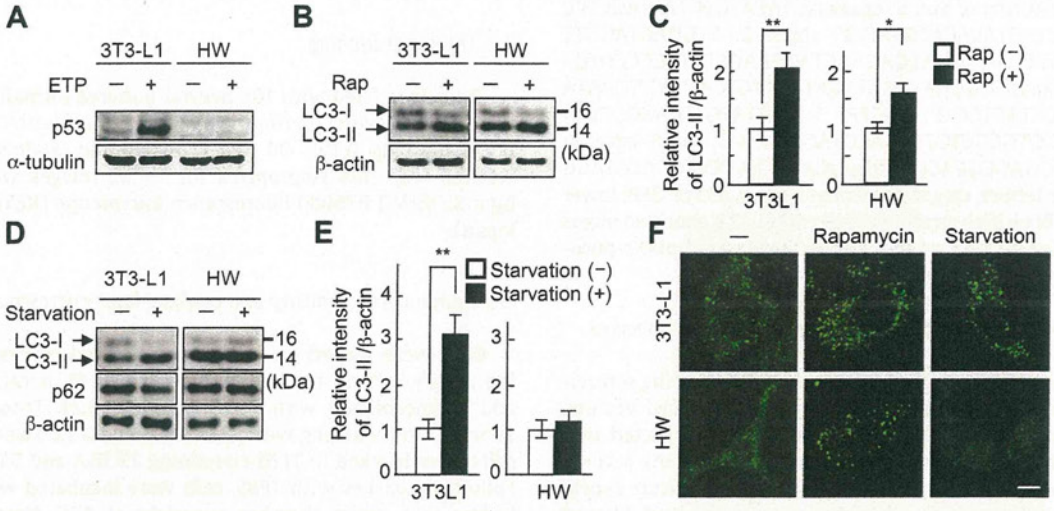

Fig. 1. p53 is required for starvation-induced autophagy. (A) 3T3-L1 and HW preadipocytes were treated with 100 μM etoposide (ETP) for 24 h. Cells were lysed and immunoblot analysis was performed using anti-p53 and anti-α-tubulin antibodies. α-Tubulin was used as a loading control. (B–E) 3T3-L1 and HW adipocytes (day 4 adipocytes) were treated with 500 nM rapamycin (Rap) for 6 h (B, C) or serum-free medium (Starvation) for 24 h (D, E). Cells were lysed and immunoblot analysis was performed with anti-LC3, anti-p62 and anti-β-actin antibodies. β-Actin was used as a loading control. The results are expressed as the relative intensity of LC3-II/β-actin compared with control cells. Values are mean ± S.D. (experiments were performed in duplicate with three independent cultures per experiment). Differences between values were analyzed by Student's *t*-test. $^{*}p < 0.05$, $^{**}p < 0.01$. (F) Immunofluorescence analysis of LC3 was performed on day 4 adipocytes. Scale bar 20 μm.

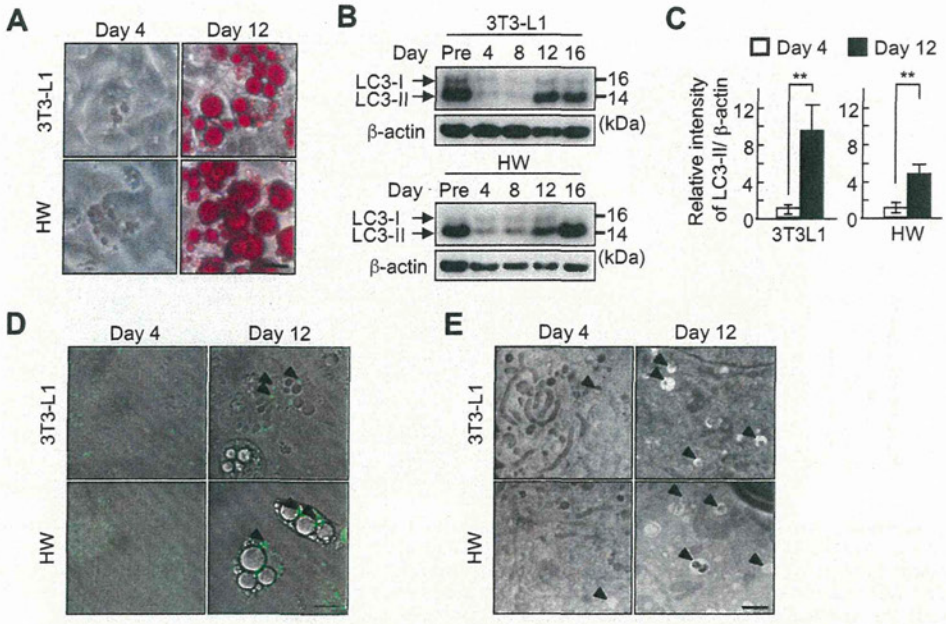

Fig. 2. Autophagy is induced in differentiated and hypertrophic 3T3-L1 and HW adipocytes. (A) Days 4 and 12 3T3-L1 and HW adipocytes were stained with Oil Red O. Scale bar 20 μm. (B) Differentiated adipocytes at the indicated time points were harvested and immunoblot analysis was performed with anti-LC3 and anti-β-actin antibodies. β-Actin was used as a loading control. (C) The results are expressed as the relative intensity of LC3-II/β-actin in day 12 hypertrophic adipocytes compared with day 4 adipocytes. Values are mean ± S.D. (experiments were performed in duplicate with three independent cultures per experiment). Differences between values were analyzed by Student's *t*-test. $^{*}p < 0.05$, $^{**}p < 0.01$. Immunofluorescence analysis with anti-LC3 antibody (D) and electron microscopy analysis (E) were performed at the indicated time points. The arrowheads point at autophagosomes and/or autolysosomes. Scale bars 20 μm and 1 μm, respectively.

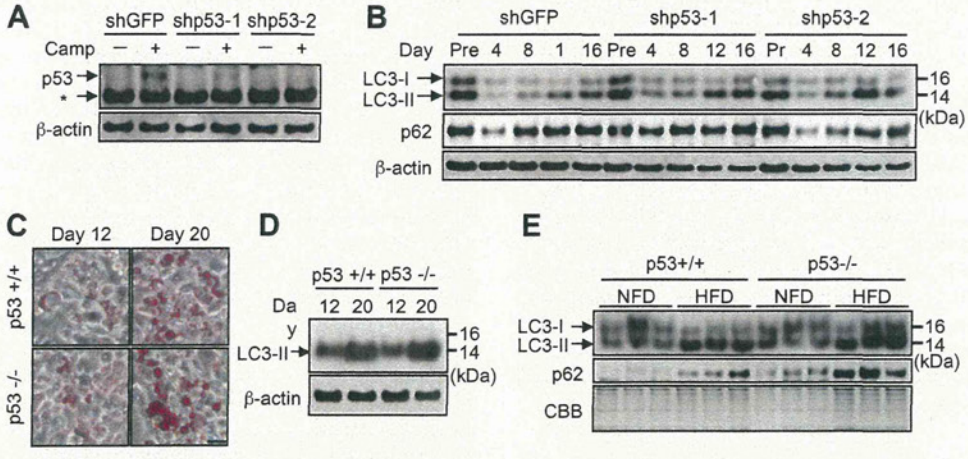

Fig. 3. p53 does not influence autophagy observed in hypertrophic adipocytes and white adipose tissue (WAT) from obese mice. (A) 3T3-L1/shGFP preadipocytes and 3T3-L1/shp53 preadipocytes were treated with 5 μM camptothecin (Camp) for 24 h. Cells were lysed and immunoblot analysis was performed using anti-p53 and anti-β-actin antibodies. β-Actin was used as a loading control. The asterisk indicates nonspecific bands. (B) The differentiated 3T3-L1/shGFP and 3T3-L1/shp53 adipocytes were harvested at the indicated time points and immunoblot analysis was performed with anti-LC3, anti-p62 and anti-β-actin antibodies. β-Actin was used as a loading control. (C, D) Differentiated $p53^{+/+}$ and $p53^{-/-}$ MEFs were stained with Oil Red O staining (C; scale bar 25 μm), or harvested at the indicated time points for immunoblot analysis with anti-LC3 antibody (D). β-Actin was used as a loading control. (E) Representative western blot of LC3. Total protein was extracted from WAT of $p53^{+/+}$ and $p53^{-/-}$ mice fed a normal-fat diet (NFD) or a high-fat diet (HFD) and immunoblot analysis was performed with anti-LC3 and anti-p62 antibodies. CBB stain was used as a loading control. The experiments were performed with 5–6 mice in each group.

To investigate whether p53 influences obesity-induced autophagy *in vivo* as well as *in vitro*, we analyzed the epididymal WAT of wild type ($p53^{+/+}$) and p53-knockout ($p53^{-/-}$) mice, which were fed an NFD or a HFD. HFD increased the body and adipose tissue weight in both mice (data not shown). Previously, it has been reported that obesity increases the expression of p53 in WAT [24,25]. In accordance with these reports, we observed that HFD-induced obesity enhanced p53 expression (data not shown). The conversion of LC3-I to LC3-II and p62 expression were dramatically and equally increased by HFD in both $p53^{+/+}$ and $p53^{-/-}$ mice (Fig. 3E), suggesting that obesity-induced autophagy in mice is regulated in a p53-independent manner as well.

3.3. Autophagic flux is suppressed in differentiated and hypertrophic adipocytes

To clarify whether the autophagic machinery is fully activated in differentiated and hypertrophic adipocytes, we compared

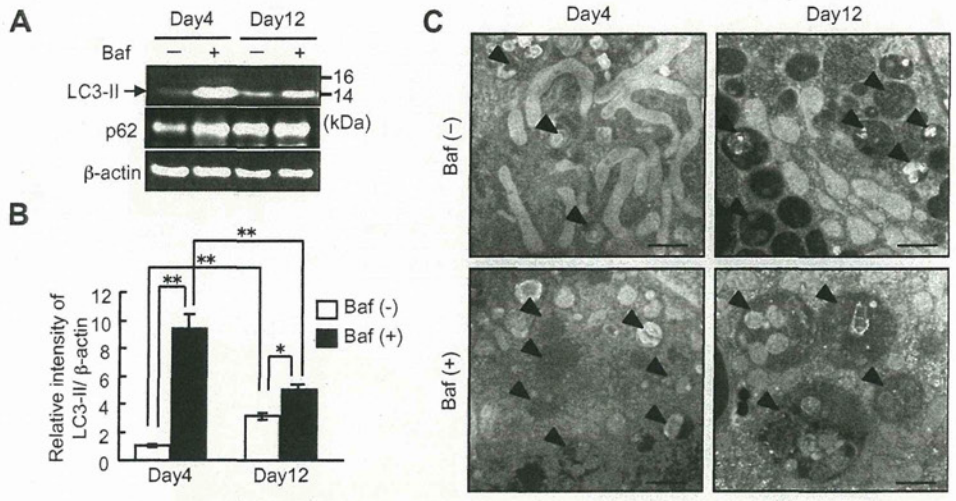

Fig. 4. Autophagic flux is suppressed in differentiated and hypertrophic adipocytes. Day 3 adipocytes and day 11 hypertrophic adipocytes were treated with 10 nM bafilomycin A1 (Baf) for 24 h. (A) Day 4 adipocytes and day 12 hypertrophic adipocytes were harvested and immunoblot analysis was performed with anti-LC3, anti-p62 and anti-β-actin antibodies. β-Actin was used as a loading control. (B) The results are expressed as the relative intensity of LC3-II/β-actin. Values are mean ± S.D. (experiments were performed in duplicate with three independent cultures per experiment). Differences between values were analyzed by Tukey–Kramer test. $^{*}p < 0.05$, $^{**}p < 0.01$. (C) Electron microscopy analysis. The arrowheads point at autophagosomes and/or autolysosomes. Scale bar 1 μm.

autophagic flux of day 12 hypertrophic 3T3-L1 adipocytes with that of day 4 3T3-L1 adipocytes. Treatment with the lysosomal inhibitor, bafilomycin A1 (Baf), significantly increased the expression of LC3-II and p62 in both day 4 adipocytes and day 12 hypertrophic adipocytes (Fig. 4A and B). Unexpectedly, however, the Baf-induced enhancement of the LC3-I to LC3-II conversion and p62 accumulation were lower in day 12 hypertrophic adipocytes than in day 4 adipocytes, suggesting that the autophagic flux was markedly suppressed in day 12 hypertrophic adipocytes compared with day 4 adipocytes (Fig. 4A and B). Using electron microscopy we observed that without Baf treatment day 12 hypertrophic adipocytes contained slightly more autophagosomes than day 4 adipocytes. The autophagosomes' size in day 12 hypertrophic adipocytes was much larger than in day 4 adipocytes (Fig. 4C). After Baf treatment, the autophagosomes' size was markedly increased in both day 4 adipocytes and day 12 hypertrophic adipocytes. Furthermore, regardless of Baf treatment, the autophagosomes containing unspecified structures, which could be undigested contents, were more frequently observed in day 12 hypertrophic adipocytes compared with day 4 adipocytes. Interestingly, unspecified structures were detected in most autophagosomes observed in day 12 hypertrophic adipocytes after Baf treatment (Fig. 4C).

4. Discussion

Previously, it has been reported that p53 is necessary for starvation-induced autophagy in MEFs, HCT116 and Saos-2 cells [7–10]. Herein, we demonstrated that p53 is necessary for starvation-induced autophagy in adipocyte cell lines (3T3-L1 and HW) as well. Electron microscopy analysis revealed that the number of autophagic vacuoles is increased in differentiated and hypertrophic 3T3-L1 adipocytes [11]. However, it has not been clarified yet whether p53 is also required for the autophagy observed in the late stage of adipocyte differentiation. Because differentiated and hypertrophic adipocytes, which accumulate large amounts of TG, may be under stress, we hypothesized that p53 is required for the autophagy observed in differentiated and hypertrophic adipocytes *in vitro* and *in vivo*. Unexpectedly, however, our findings suggest that autophagy observed in differentiated and hypertrophic adipocytes is p53-independent.

Here, we also evaluated the autophagic flux of day 4 adipocytes and day 12 hypertrophic adipocytes, and found that it was markedly suppressed in day 12 hypertrophic adipocytes compared with day 4 adipocytes (Fig. 4A and B). The autophagic machinery consists of three major steps, autophagosome formation, autolysosome formation and degradation of autolysosome contents. During the autolysosome formation, the autophagosome fuses with a lysosome containing many hydrolases. Lieberman et al. [26] hypothesized that lysosomal dysfunction could be seen primarily as autophagy disorder in several types of lysosomal storage diseases. Our electron microscopy analysis of day 12 hypertrophic adipocytes clearly indicated that the autophagosome increases in size and certain structures remain undigested in the autophagosome, and that Baf-treatment enhances the hypertrophy-associated changes. Based on the above-mentioned hypothesis, our data suggest that either autolysosome formation or lysosome function may be impaired in differentiated and hypertrophic adipocytes. Recently, using GFP-LC3 transgenic mice with the lysosome inhibitor, chloroquine, it has been shown that autophagy is suppressed in obese WAT. Moreover, autophagy regulates the inflammatory response in hypertrophic adipocytes [27]. Therefore, we suggest the possibility that autolysosome formation and/or lysosome functions may be impaired in hypertrophic adipocytes *in vitro* and *in vivo*, and the autophagic machinery may be a novel therapeutic target for adipocyte inflammation in obesity and type 2 diabetes.

Acknowledgments

We thank all members of the Molecular Pathology and Metabolic Disease, Animal Center of the Faculty of Pharmaceutical Sciences, Tokyo University of Science, for their cooperation. We thank Dr. Miyoko Irie and Professor Ken Takeda in Hygienic Chemistry, Faculty of Pharmaceutical Sciences, Tokyo University of Science, for their invaluable technical assistance. We also thank Professor Shigeomi Shimizu from Tokyo Medical and Dental University for his helpful suggestions. This work was partially supported by Kyorin Pharmaceutical Co., Ltd.

References

[1] B. Levine, G. Kroemer, Autophagy in the pathogenesis of disease, Cell 132 (2008) 27–42.